Laya, J. C., Sulaica, J., Teoh, C. P., Whitaker, F., Gabellone, T., Tucker, M. E., Tesch, P., Miller, B., Prince, K., & Izaguirre, I. (2018). Controls on Neogene carbonate facies and stratigraphic architecture of an isolated carbonate platform – the Caribbean island of Bonaire. *Marine and Petroleum Geology*, *94*, 1-18. https://doi.org/10.1016/j.marpetgeo.2018.03.031

Controls on Neogene carbonate facies and stratigraphic architecture of an isolated carbonate platform – the Caribbean island of Bonaire

Juan Carlos Laya[1], Jonathan Sulaica[1], Chia Pei Teoh[1], Fiona Whitaker[2], Tatyana Gabellone[2], Maurice Tucker[2], Philipp Tesch[1], Brent Miller[1], Kieron Prince[1], Ingrid Izaguirre[3]

[1]Department of Geology & Geophysics, Texas A&M University, TAMU 3115, College Station, TX, 77843-3115. USA

[2]School of Earth Sciences, University of Bristol, Bristol BS8 1RJ, UK

[3]Neptune Isotope Laboratory (NIL), Division of Marine Geology and Geophysics, Rosenstiel School of Marine and Atmospheric Science (RSMAS), the University of Miami, 4600 Rickenbacker Causeway, Miami, FL, 33149, USA

*e-mail: layajc@geos.tamu.edu

Abstract

The Neogene carbonate succession on the island of Bonaire (Netherland Antilles) shows complex geometries associated with a sequence of depositional and erosional events which reflects the history of this isolated platform and the interaction between eustasy and tectonics. Three major episodes of carbonate platform deposition are defined which show contrasting depositional styles: 1) aggradational platform (Lower-Middle Miocene) with sediments showing a fining-upward trend from mixed coral rudstone to medium-grained coralgal grain/packstone, partly dolomitized and tilted by tectonic deformation; 2)

prograding platform (Upper Miocene-Pliocene) which is formed of several shallowing-upward prograding units mainly composed of reworked red algal grain/packstone, with significant dolomitization, passing upward to shoreline and aeolian deposits formed of coralgal grain/packstone and large benthic foraminifera grainstone, and 3) flat-topped platform (Pleistocene) with a reefal framework composed of a rich variety of corals in a bioclastic pack/wackestone matrix. These platform episodes exhibit contrasting stacking patterns and are separated by erosional unconformities. Overprinting this depositional succession is a series of Quaternary near-horizontal shoreline erosional terraces and vertical cliffs which have been cut into the island stratigraphy and complicate the stratal field relationships. However, this terrace morphology clearly does not represent depositional episodes, as has been suggested before. The internal architecture of each of the three carbonate platform episodes reflects interaction of the dynamics of sedimentation with allogenic controls. The latter relate to major oceanographic and tectonic events in the region, including changing ocean circulation as a result of the closure of the Panama isthmus, and Caribbean plate dynamics that affected sea-floor and island topography. The Bonaire succession provides a model for understanding and predicting isolated carbonate platform development, as well as architecture, facies and potential diagenetic changes, in an active tectonic setting.

Keywords

Neogene; carbonate platform; allogenic controls; facies; ocean circulation; red algae; Caribbean; Bonaire Island;

1 Introduction

Cenozoic isolated carbonate platforms around the globe have been described by many authors (e.g. Bosence, 2005; Pomar, 2001; Pomar and Hallock, 2008). These platforms usually contain a large variety of flora and fauna, but are commonly dominated by corals, coralline algae and large benthic foraminifera (Braga et al., 2010). During the Miocene, several climatic and oceanographic events occurred which had a significant impact on carbonate production, including the Miocene Climatic Optimum 17 - 14.7 Ma and the subsequent major climatic shift to cooler temperatures *circa* 14 – 11 Ma that led to the transition to the present-day climate (Betzler et al., 2016; Holbourn et al., 2015). Additionally, the uplift and closure of the Panama Isthmus and associated regional tectonic events (4.6 - 3.6 Ma) (Haug and Tiedemann, 1998; Reijmer et al., 2002; Schneider and Schmittner, 2006) resulted in significant alteration of ocean circulation patterns and nutrient supply, both of which are important factors for carbonate production.

Regional-scale carbonate platform architecture has been studied extensively (e.g. Della Porta et al., 2004; Eberli and Ginsburg, 1989; Kenter, 1990; Pomar, 1991), along with stratal geometries and their authigenic controls, including hydrodynamics and ecological factors (Pomar and Kendall, 2008). However, most studies have focused on platforms within tectonically stable regions (e.g. the Bahamas), where carbonate production and stratigraphic architecture are primarily governed by sea-level history and environmental factors. The relatively few studies of platform evolution in tectonically active settings (e.g. Matthews, 1968; McNeill et al., 2012; Pedoja et al., 2014) mostly focus on coastal margins and island evolution associated with faults or passive margin-opening ocean locations, such

as the Red Sea (Purser and Bosence, 1998) where syn-sedimentary faulting is the important control.

The island of Bonaire, in the Southern Caribbean, presents a spectacular set of outcrops that make it an ideal location to understand the effects of interactions between sea-level change, oceanographic circulation, climate and tectonic forces on platform evolution. Bonaire, located some 90 km north of Venezuela (Fig. 1), is one of the three islands that comprise the Netherland or Leeward Antilles, also known as the ABC islands (Aruba, Bonaire and Curaçao).

Earlier studies have identified the stratigraphic significance of Cenozoic sea-level variations and especially of tectonic activity related to the interaction of the South American and Caribbean plates (Deffeyes et al., 1965; Engel et al., 2013; Hippolyte and Mann, 2011; Schellmann et al., 2004). The sum of these processes has created an onlapping depositional pattern with an apparent inverse stratigraphy, in which the youngest units occur at the lowest elevations on the island, with the older strata mostly located at higher elevations. All this variation occurred without any obvious influence from folding or faulting.

Many authors have described the surficial terrace morphology of the ABC islands, including Bonaire, as the product of subaerial exposure and coastal erosion during Quaternary interglacial highstands (e.g. Alexander, 1961; Bandoian and Murray, 1974; De Buisonjé, 1963, 1974; Muhs et al., 2012; Schellmann et al., 2004). However, there is a lack of consensus in both description and interpretation of the depositional units of Bonaire. This includes the number of terraces present on the island, as well as their correlation with those

on Curaçao and Aruba, where between 3 and 7 different terraces have been recognized, respectively (Alexander, 1961; Bandoian and Murray, 1974; De Buisonjé, 1974; Kim and Lee, 1999). Here we present evidence demonstrating that the erosional features provide less stratigraphic information than has been suggested before. We show instead that the depositional episodes can be better understood by focusing on the internal architecture of the strata and their regional trends.

This paper aims to document the internal geometries of the platforms of Bonaire and their relationship with facies to refine the Neogene stratigraphy of the island, to serve as example of an isolated carbonate platform in an active tectonic setting. We consider the platform evolution in a regional context, to understand the interaction between sedimentation dynamics and allogenic controls, including changing climate and the effect of regional tectonics on relative sea-level and ocean circulation. We postulate that the regional eastward tectonic front has dominated the macroscale facies development, as well as the meter-scale internal architecture of the facies. This new interpretation has implications for facies geometry trends for similar stratigraphic architectures in other isolated platforms in the Caribbean (e.g. Barbados, Dominican Republic and Jamaica) and tropical regions elsewhere around the world which have been influenced by the interplay of these same controls. In addition, it provides a foundation for study of trends in diagenetic overprint, in particular the development of dolomitized horizons within the Bonaire carbonates, which will be discussed in detail in a subsequent paper.

2 Geological background

Over the last 80 Ma, the region north of Venezuela has been dominated by the Caribbean Plate interacting with the surrounding plates and moving eastwards, relative to South America, near-continuously from the Cretaceous to the present-day (Escalona and Mann, 2011; Jordan, 1975; Pérez et al., 2001; Pindell et al., 1988; Trenkamp et al., 2002). This movement has created transtensional, transpressional and convergent plate boundaries, giving rise to tectonic subsidence and uplift. To the east, subduction of the convergent plate boundary has created the volcanic island arc of the Greater and Lesser Antilles, whereas the southern boundary near the ABC islands experienced transtensional and transpressional forces(Escalona and Mann, 2011).

The island of Bonaire is characterized by Cretaceous volcanic basement rocks, limited Eocene clastics (Soebi Blanco Fm.), overlain by Miocene-Pliocene carbonates (Seroe Domi Fm.), and finally Pleistocene-Holocene shallow-marine carbonates (Bandoian and Murray, 1974; De Buisonjé, 1974; Hippolyte and Mann, 2011; Pijpers, 1933) (Fig. 2). Cretaceous volcanic rocks of the Washikemba Fm. form the basement and are composed of rhyolite and dacite, which have been radiometrically-dated at ~90 Ma using $^{40/39}$Ar (Thompson et al., 2004; Van Der Lelij et al., 2010).

In most places the Miocene Seroe Domi Fm. directly overlies the volcanic basement and can be correlated with Miocene carbonates on Aruba and Curaçao. The Middle-Lower Miocene succession displays a high-angle dip up to ~30° degrees southeast away from the inner part of the island (Fig. 2) (Hippolyte and Mann, 2011). Overlying, but as part of Seroe Domi Fm., are late Miocene-Pliocene carbonates, formed of large benthic foraminifera, coralline red

algae and rare fragments of gastropods, bivalves and corals. The erosional terraces occur mainly on the eastward (windward) side of the island, and they were initially interpreted as erosional features cutting into Pleistocene reefal carbonates (Alexander, 1961; Bandoian and Murray, 1974; Herweijer et al., 1977; Herweijer and Focke, 1978). Here we present evidence suggesting that these terraces also expose Miocene strata and that their morphology is partly independent of the stratigraphy.

Situated at 13°N latitude, Bonaire is at present bathed in warm tropical waters throughout the year, ensuring optimal conditions for coral reef growth. However, before the closure of the Panama Isthmus during the Mid Pliocene, a constant high nutrient supply from the Pacific Ocean may have restricted the development of coral communities, allowing organisms such coralline red algae to dominate shallow-marine carbonate production (Budd et al., 1998; Reijmer et al., 2002). The present-day climate is semi-arid, with an annual rainfall of approximately 55 cm yr^{-1} and an average temperature of 27ºC (Martis et al., 2002). Average temperature and precipitation rates may have been different during the Neogene, as a result of the migration of the intertropical convergence zone (ITCZ) and changes in the global climatic regime. Thus, from the Miocene Climate Optimum the climate cooled progressively during the Upper Miocene to the present (Chiang and Bitz, 2005). During the Pleistocene higher frequency climatic oscillations have been proposed, driven by orbital insolation changes (Felis et al., 2015).

High-energy waves impact the eastern side of the island as a result of the persistent trade winds (Haug and Tiedemann, 1998; Nisancioglu et al., 2003), which also drive the marine current system in the area. Tides within the Leeward Antilles are microtidal, with a range of

approximately 30 cm, and this provides the stability for extensive coral-reef growth (Lorscheid et al., 2017). Nutrients at the present-time, derived mainly from the Amazon and Orinoco rivers (Hu et al., 2004), are being provided from the south through the surface current as well as, from upwelling in some areas.

3 Data and Methods

Traditional field mapping, in conjunction with GigaPan© photo mosaics and drone-based photogrammetry have been used to construct digital outcrop models and high-resolution maps to reveal the stratigraphic architecture and facies distribution on Bonaire. In addition, a total of 235 samples were collected to record lateral and vertical variability in facies and mineralogy. 51 hand samples and 184 short (12 to 45 cm length, 2-in diameter) cores were acquired from multiple locations on Bonaire to sample the three main carbonate platform stages. The 2-inch diameter cores were collected using a Tanaka TED-270PFDH dual-handle gas-powered core drill. High-resolution orthomosaics and GigaPan© Images were prepared for stratigraphic architecture.

A facies scheme was produced based on field observations, sample descriptions, petrography and mineralogical data. Petrographic images were captured with an Olympus BX53MTRF microscope using Olympus Stream Essentials 2.1 software. Dunham (1962) carbonate rock classification, as modified by Embry and Klovan (1971), was used to define facies/microfacies.

$^{87}Sr/^{86}Sr$ isotope analyses, used here to constrain ages by comparison with the global sea-water curve were conducted at the Texas A&M University R. Ken Williams Radiogenic

Isotope Geosciences Laboratory. In view of absence of molluscs, brachiopods and oyster shells, samples of uniform unaltered carbonate material were used. Mainly muddy carbonate sediments and early dolomites were selected and screened for this analysis. Bulk samples were used, but as Edwards et al. (2015) suggests that preserved bulk carbonates can be used for Sr isotope stratigraphy. During the procedure cements and calcite veins were avoided and X-ray diffraction was carried out in the Department of Soil and Crops at Texas A&M University to quantify the mineralogy for the selected sample set; a small sample sub-set was analyzed in the Carbonate Petrology and Characterization Laboratory at Western Michigan University.

Samples were crushed by agate pestle and mortar and approximately 10-100 mg of powder were dissolved with 6M HCl in sealed Teflon beakers on a 90°C hot plate overnight. The HCl solution was evaporated and converted to HNO_3 solution for chemical purification on 100 µl of Sr-Spec resin. Purified solutions were loaded on outgassed Re filaments with a TaO emitter solution.

Mass spectrometry was conducted on a Thermo Scientific Triton thermal ionization mass spectrometer running in static multiple-Faraday detector mode with amplifier rotation. Ion beams were in general 8-15 V of ^{88}Sr measured on $10^{10}\,\Omega$ resistors. Analyses consisted of ten to twenty-five blocks of 15 two-second integrated cycles with outlier exclusion of points greater than 2 standard deviations from the mean. Measured isotope ratios were normalized to $^{88}Sr/^{86}Sr=8.375209$. Fourteen replicate analyses of NIST 987, conducted during sample analyses, yielded an average $^{87}Sr/^{86}Sr$ of 0.710235 and an external reproducibility of 5.3 ppm. Internal precision of $^{87}Sr/^{86}Sr$ was better for most samples; diagrams were plotted and

calculations conducted with this external reproducibility unless the internal measurement precision was greater than 5.3 ppm, in which case the measurement precision was used. The age model was produced based on the Sr isotope curve from McArthur et al. (2012).

In addition, 9 samples of coral fragments (*Montastrea annularis* and *Diploria strigose)* were dated with U-Th at the Neptune Isotope Lab (NIL), the University of Miami, RSMAS. Screening using XRD showed these were dominantly aragonite, except for one sample of 100% low-Mg calcite. The Neptune Isotope Lab used 0.15 grams of the carbonate samples provided in the Uranium Thorium geochronological dating. Each powdered sample was dissolved in 3.5 mL of HNO3 acid before being spiked with 0.5 g of the ^{229}Th-^{233}U-^{236}U spike mixture. 0.2 mL of concentrated HNO_3 was added to the vials in order to compensate for the added spike. In order to separate the Uranium and Thorium for further analysis, the samples were eluted using a U/TEVA resin designed to remove the matrix within the sample and successfully separate the Uranium and Thorium. The resin was treated with 10 mL of 0.1 mol HCl in order to remove any background trace amounts of U/Th from previous runs. Two sets of 10 mL of 6 mol. HNO_3 was then eluted at a rate of 1 mL / minute in order to remove the matrix elements. 5 mL of 3 mol. HCl was then added to the column in two batches in order to collect the Thorium portion of the sample. 5 mL of 0.1 mol. HCl was then used to elute and collect the Uranium portion of the sample in separate vials. The solutions were evaporated at 60–100 °C in a fume hood before analysis. The samples were then run through the ThermoFisher Neptune Plus Multi Collector-Inductively Coupled Plasma-Mass Spectroscopy. The data collected was processed through an open-source algorithm in Mathematica which calculates an accurate age while taking all sources of uncertainty

contribution into consideration.

Stable isotope carbon ($\delta^{13}C$) and oxygen ($\delta^{18}O$) isotopes and trace element analysis was carried out on selected samples. The stable isotope measurements were performed using a Kiel IV carbonate device coupled to a Thermo-Scientific MAT 253 isotope ratio mass spectrometer in the Stable Isotope Geosciences Facility at Texas A&M University. The results are reported in VPDB standard with an analytical precision of 0.04‰ for $\delta^{13}C$ and 0.08‰ for $\delta^{18}O$. Major and trace element analyses including aluminum (Al), strontium (Sr), manganese (Mn) and iron (Fe), reported in parts per million (ppm), were determined by an ICP-MS in the Radiogenic Isotope Geosciences Laboratory of Texas A&M University. Precision of major and trace element analysis was 0.001 ppm for Sr, 0.003 ppm for Mn and 0.03 ppm for Fe.

4 Facies Analysis

We recognize three episodes of Neogene platform development on Bonaire, separated by unconformities and having distinct depositional styles: 1) An aggradational platform (Middle Miocene), 2) a progradational platform (Upper Miocene-Pliocene), and 3) a flat-topped reefal-dominated platform (Pleistocene). These platforms show contrasting facies associations and a scheme is presented below for each platform and briefly described in Table 1 and Figure 3.

4.1 Facies distribution and platform architecture

The Middle-Lower Miocene aggradational platform is a well-bedded succession that represents the initial stage of Miocene sedimentation in the region. These carbonates can be correlated to the tilted strata on Curaçao and Aruba (Alexander, 1961; De Buisonjé, 1974;

Deffeyes et al., 1964; Fouke et al., 1996; Sibley, 1980). The strata are restricted to the northwestern part of the island (Fig. 2) and show a thickness of ~60 m. The best documented outcrops are at Goto Meer and Dos Poos. The Goto Meer exposure is a reference outcrop for this platform, which shows an overall fining-upward trend from *mixed coral rudstone* to medium-grained *coralgal grain/packstone* (Fig. 4). The contact between the first Miocene Platform and Upper Miocene-Pliocene deposits is an angular unconformity that has only been recognized in the Goto Meer outcrop close to Rincon Town.

Overlying the aggradational platform is the Upper Miocene-Pliocene prograding platform which exhibits a more complex geometry, including clinoforms and a series of onlap and toplap terminations (e.g. Fig 5). Outcrops of the prograding platform are distributed across the center of the island and are limited to the east by a boundary with the younger platform (Fig. 2). Four facies form this platform (Fig 6): 1) *coralgal grain/packstone* (Fig 6A), 2) *encrusting red algae-rich and rhodolite grainstone/packstone* (Fig 6B, 6C, 6G), 3) reworked *red algal grain*/*packstone* (Fig. 6D), and 4) aeolian deposits with *large benthic foraminiferal grainstone* (Fig 7). Facies descriptions and interpreted environment of deposition are summarized in Table 1. Reef-building corals are completely absent in most outcrops, and where they do occur are broken and reworked.

In outcrops such as Seru Grandi and Boca Onima (Fig. 5 and 6), the platform shows sigmoidal bed-geometries with angles up to 12º and a consistent eastward progradational trend and variable elevation between ~18 and ~70 m above sea-level; in addition, aeolian deposits can reach up to 100 m in elevation in localities such as Seru Largu. The contact surface is a well-defined erosional unconformity which can be observed in the Seru Grandi

outcrop in the northern part of the island (Fig. 5, 6E, 6G and 6F). A recent detailed ground penetrating radar (GPR) survey carried out by Bowling et al. (in revision) has revealed the orientation and frequency of bedding within this platform across the central and northern side of the island. The bed orientation pattern shows complex internal stratigraphic relationbships which correspond with our interpretation of allogenic controls driving the main geometries of the different platform stages.

The younger Pleistocene platform has a flat-topped geometry, forming a reefal rim around most of the island. On the northern side of Bonaire these deposits extend to approximately 8 m above sea level, whereas the same strata on the southern side of the island lie beneath the modern lagoons of Pekelmeer and Lac Bai, which are characterized by recent microbial-evaporitic carbonate deposits (Lucia, 1968; Sibley and Murray, 1972). On the eastern side of the island the Pleistocene platform includes an additional thin, ± 5 m thick, stratal package that forms the second terrace with elevation ranging from 15 to 30 m above sea-level. This platform comprises massive and poorly-bedded deposits dominated by reefal facies with *Montastrea*-rich boundstone, *Acropora cervicornis* floatstone and *Montastrea*-rich *rudstone;* many of the corals can be observed to be in growth position (Fig. 8, 9, 10). Bioclastic deposits filling cavities between reefal structures include Gastropod-green algal grainstone/packstone and Coralgal grainstone/packstone (Fig 9). In addition, encrusting coralline algae are binding the bioclastic material in some of the deposits; these could well have originated during the Holocene, as also shown by Rixhon et al. (2018) (Fig. 10).

5 Age constraints on deposition of the three carbonate platforms

$^{87}Sr/^{86}Sr$ values of the carbonate rocks on Bonaire vary between 0.7083 and 0.7092. The

values were plotted on the global $^{87}Sr/^{86}Sr$ curve of McArthur et al. (2012) to generate reference ages (Fig. 11). The aggradational platform gives values between 0.7083 and 0.7084 for the lowest part of the section, deposited on top of the volcanic basement, with similar values for the middle part of the succession. These $^{87}Sr/^{86}Sr$ values indicate that this platform stage consists of the oldest Miocene deposits on the island, with ages within the Lower Miocene (Table 2). This platform may correspond to the basal unit of the Seroe Domi Formation assigned by Fouke et al. (1996) as subunit 1 and dated as Middle Miocene. Although the $^{87}Sr/^{86}Sr$ values from the aggradational platform are consistent, they are lower than those for subunit 1 (Fouke et al., 1996) and thus present older values. This may be the result of contamination by volcanic material that may have provided strontium from the basaltic rocks. One sample in this platform stage deposit shows an $^{87}Sr/^{86}Sr$ value of 0.708988 corresponding to a younger age of only 6 Ma. This result could reflect a resetting of $^{87}Sr/^{86}Sr$ values by dolomitization during the Late Miocene-Early Pliocene which affected the older carbonates on the island (Fig. 11).

Samples from the prograding platform display a broader range of $^{87}Sr/^{86}Sr$ values which vary between from 0.7088 and 0.7090 (Table 2) yielding ages mostly between 4 and 10 Ma, with 2 outliers that give Middle Miocene ages. A variety of materials were analyzed including skeletal grains and fully dolomitized samples. This platform appears to correlate well to Fouke et al. (1996)'s subunit 2 which extends from the Upper Miocene to Lower Pliocene, i.e. from 10-5 Ma (Fig12) (Budd et al., 1998; Fouke et al., 1996). These age results suggest that there are Miocene deposits within the carbonate terraces that were previously considered to be of Pleistocene age by many authors (i.e. Alexander, 1961; Bandoian and Murray,

1974; De Buisonjé, 1963, 1974; Muhs et al., 2012; Schellmann et al., 2004).

The youngest flat-topped platform yielded $^{87}Sr/^{86}Sr$ values between 0.7091 and 0.7092, suggesting younger (Pleistocene) ages for these deposits. In addition, U-Th dates on corals show a range from ~715 Ky to ~115 Ky (Table 2). The younger platform strata correspond to the morphology of the first terrace and eastern part of the second terrace with an elevation above sea-level of between 8 m and 15 m, respectively. Both windward and leeward terraces distinctly cut into the Pleistocene carbonates. A wave-cut notch is readily identifiable at approximately ~2 m above sea-level on the leeward (western) side of the island and ~10 m above sea-level on the windward side. According to the U-Th values of the samples the first terrace (elevation 8 m) has an age of 126 +/- 6 Ky (n=8, excluding one outlier at 198 Ky), which corresponds to MIS 5e. The mineralogy within this platform stage is still the original aragonite, with minor calcite-rich facies. Our results presented here agree with Obert et al. (2016) and Rixhon et al. (2018) who dated coral samples from the first terrace on Bonaire, and also with Schellmann et al. (2004)and Muhs et al. (2012) who analyzed samples from the correlative deposits in Curaçao using Electron Spin Resonance (ESR) and Uranium-series dating, respectively. All of these studies obtained dates approximating to 125 Ky, which coincides with the MIS 5e interglacial period and the results of this study. The second young terrace (elevation 10-15 m) is dated by a single sample at 715 Ky, which may correspond to MIS 15-17 (Hornbach et al., 2010; Lisiecki and Raymo, 2005; Muhs et al., 2012; Waelbroeck et al., 2002), rather older than suggested by Muhs et al. (2012) who ascribed this to MIS 11-13 (~400-500 ky). However, this values can be questioned due to the nature of the sample (low-Mg calcite) and the fact that it is out of the accepted range for U-Th dating

techniques. For that reason we are less confidence in this result.

6 Depositional environments and Stratigraphy

6.1 Aggradational platform deposits (Lower-Middle Miocene)

Overall, the succession shows a fining- or deepening-upward trend which is composed of reworked coral rudstone reflecting high-energy conditions, and grainstone deposited under quieter conditions. The presence of light-dependent organisms such as coral and green algae at the base of the succession suggests warm and very shallow waters. However, most of the skeletal grains are not in growth position; instead, they are mostly composed of broken fragments and reworked material in coarse bioclastic facies. These characteristics indicate significant fragmentation and abrasion by wave action in very shallow water (Pomar et al., 2012; Pomar et al., 2015). In addition, there are no in-situ reefal frameworks, implying that the shallow conditions were not favorable for reef development. Thus, corals and other euphotic organisms lived disseminated across a hard substrate, heavily affected by strong fair-weather wave action. Passing upwards, a mixed bioclastic grain/packstone facies suggests changes in light penetration to more oligophotic conditions. Similar fragmentation and reworking of skeletal material in the Miocene carbonates of the Perla oil-field in Venezuela, located 230 km southwest of Bonaire, are ascribed by Pomar et al. (2015) to internal wave action.

The bed-stacking pattern shows a thinning-upwards sequence, but the mainly uniform meter-scale bedding could suggest that deposition took place on a relatively flat surface of a flat-topped isolated platform or perhaps an open lagoon behind a thin, poorly-developed reef or storm coastal barrier. However, bedding planes show irregular and locally wavy structures,

mainly in coarse skeletal debris, which indicate localized wave action. Stratal thickness may have been controlled by accommodation and the nature of the carbonate factory. The latter is mainly composed of autotrophic and mixotrophic organisms such coral, gastropod, bivalves and green algae, passing upwards into deposits dominated by heterotrophic organisms, including echinoids and large benthic foraminifera with some autotrophic organisms such as red algae (James, 1997; Pomar et al., 2015; Schlager, 2003) (Fig. 4).

6.2 Prograding platform deposits (Upper Miocene- Pliocene)

This platform stage is composed mainly of calcareous red algae which form up to 70% of the sediment, with minor components of large benthic foraminifera, limited coral fragments, lithic grains, echinoids and rare molluscs. The most common encrusting coralline red algae include *Sporolithon* sp., *Spongites* sp., *Lithothamnion* sp. and *Neogoniolithon* sp. This skeletal material is different from that of typical low-latitude carbonate platforms which are dominated by the tropical carbonate factory (euphotic shallow-water organisms such as green calcareous algae and corals). Prograding clinoforms are the dominant geometries in this depositional package, in which facies change laterally and vertically from encrusting rhodolites at the upper part of the clinoforms to more bioclastic reworked material laterlly downward (Fig. 5). In fact, individual clinoform beds show almost exclusively encrusting red algae and rhodolite facies in the upper part of the section, grading laterally downslope to reworked bioclastic material with mixed lithic fragments, large benthic foraminifera commonly *Amphistegina sp., Cycloclypeus* and Miogypsinids, along with abundant rounded red algal fragments (Fig. 6).

During this depositional stage, accommodation would have been limited to the platform top,

forcing sediments to be shed laterally towards the open sea, to form the wedge-like beds and the overall clinoform geometry of this platform margin (Schlager et al., 1994). The nature of the sediments (encrusting rhodolites, reworked red algal fragments and large benthic foraminifera) suggests deposition in the oligophotic zone (Pomar et al., 2012; Pomar et al., 2015) with evidence to suggest slightly deeper water. During the Neogene, examples of carbonate production by non-framework building, light-dependent biota have been reported (Courgeon et al., 2016; Courgeon et al., 2017; Pomar et al., 2015; Wilson and Vecsei, 2005). However, on Bonaire these deposits pass laterally westwards to shoreline and aeolianite facies which suggests that they are probably shallower than proposed for similar facies in other localities such as the Perla oil-field, Venezuela(Pomar et al., 2015) (Fig. 12). This interpretation may indicate that water on the platform was not as clear as envisaged in the classic tropical factory model, or that excess nutrients restricted the growth of reef framework corals (Fig. 12). Most of the upper parts of the clinoform facies are partly to completely dolomitized, with the degree of dolomitization decreasing down the clinoform beds (Laya et al., 2017). In the type outcrop (Seru Grandi), clinoforms show a well-defined cyclic thickening upwards trend from ~2 m to ~5 m as the most common arrangement; however, the clinoforms increase in thickness eastwards, reaching up to 11 m. The presence of clastic components within the carbonate facies at more westward locations is evidence of a more proximal influence. These rounded sand- and gravel-sized lithic fragments are formed of volcaniclastic material derived from the igneous basement which support our interpretation of a high-energy environment.

Laterally, the facies pass into fine, well-sorted grainstone with large and high-angle (>30º)

cross-bedding, exposed in the central part of Bonaire (in the vicinity of the Seru Largu Millennium Monument) (Fig. 7). This grainstone is composed of well-rounded bioclasts, mainly of benthic foraminifera (*Amphistegina sp.*), bryozoans and bivalves, and reaches up to 40 m in thickness. These beds, interpreted as aeolianite dunes, are the topographically highest carbonate strata on the island. This deposit possesses most of the features that Frébourg et al. (2008) suggested are indicative of aeolianite strata, including high-angle cross-stratification and a dominant grainstone texture, as well as rounded and well-sorted grains. These sediments may have been derived from beaches located along the windward coast, as suggested by De Buisonjé (1974). The grains were carried by the strong and constant trade winds from the east and deposited in the center of the island. They form elongate, curved geobodies, ranging in area from 0.01 to 0.35 km^2 and perpendicular to the preferential wind direction, with the long axis oriented ~20° northeast-southwest. During sea-level highstands these deposits probably formed low sandy paleo-islands in the platform center (Fig. 3, 7 and 12). It might be expected that this facies should show evidence of vadose diagenesis as it was subjected to a lengthy period of exposure. No vadose cements have been identified, although meteoric isotopic signals have been reported by Sulaica (2015) with negative values of both $\delta^{13}C$ and $\delta^{18}O$. The lack of significant meteoric cementation is likely the result of the semi-arid climate that Bonaire Island has experienced since the Miocene.

6.3 Flat-topped platform deposits (Pleistocene)

This stage is dominated by a reefal framework structure formed of a rich variety of corals. The predominant species in these reefs are hermatypic corals, which are abundant throughout the modern Caribbean Sea (Milliman, 1974; Stehli and Wells, 1971; Wells, 1957). Abundant

coral species in these deposits include *Montastrea annularis, Acropora palmata, A. cervicornis, Diploria clivosa, D. labrinthiformis, Porites porites, P. astroides, Siderastrea sidera, S. radian* and *Agaricia agaricites* (Bak, 1977; De Buisonjé, 1974; Kim and Lee, 1999; Pandolfi and Jackson, 2001; van Duyl, 1985). A high degree of encrustation by coralline red algae and foraminifera, up to 10 cm thick, is present around most of the coral fragments, and this is best developed in the upper-most part of the flat-topped section, especially in the coral rubble facies (Fig. 10). One of the most important controls in the coral distribution is wind-driven wave action, which would have limited the location of coral species. Pandolfi and Jackson (2001) described similar coral assemblages from the Curaçao Pleistocene reefs (Fig. 13). In Bonaire, this youngest platform is extensively developed around the island, whereas on the eastern side it is dominated by head corals *Montastrea* sp. and *Diploria* sp. that indicate a windward back-reef setting (Dustan, 1975; Pandolfi and Jackson, 2001).

Although, small colonies of the robust *Acropora palmata* are present that can be interpreted as reef crest, these are mostly restricted to the windward side of the island. The floatstone facies, consisting of delicate branching coral *Acropora cervicornis* in a bioclastic matrix, is restricted to the leeward side of the island, indicating a protected depositional environment with relatively lower energy on the reef crest (James et al., 2010; James and Jones, 2015) (Fig. 14). The geometries of the flat-topped platform deposits show a wedge like structure with a ~10 m height that pinches out landwards. These reefal deposits are located in the coastal areas and they extend from 300 m up to 2 km inland. Reefal deposits vary from well-developed reef structures (single coral heads up to 3 m across) to grainier (sand-size)

bioclastic facies inland. The dynamics of deposition are interpreted as being dominated by storm events, with enough energy to rework significant volumes of reef-derived material on the windward side of the island.

The Pleistocene stratigraphy on Bonaire has been interpreted as directly related to glacio-eustatic sea-level changes, as well as tectonic uplift, as has also been the case with studies on Curaçao (Bandoian and Murray, 1974; Escalona and Mann, 2011; Hippolyte and Mann, 2011; Muhs et al., 2012). However, the results of this research suggest that only two stages of Pleistocene highstand are recorded here: MIS 5e stage (~ 125 ky) and MIS 13 or 17 (~500 to 700 ky), since most of the deposits in the higher terraces in the central platform have yielded $^{87}Sr/^{86}Sr$ dates indicating an upper Miocene-Pliocene age. The contrasting styles in deposition and stratigraphic architecture are strong arguments to support these interpretations.

7 Geometries and stratigraphic architecture

During the evolution of Bonaire, a range of processes controlled the geometries of the carbonate deposits and their stratal architecture. The initial deposits are a well-bedded succession that indicate deposition on a horizontal flat-topped shelf, which was then tilted as a result of a tectonic compression (Hippolyte and Mann, 2011; Pijpers, 1933). Earlier work by De Buisonjé (1974) and Deffeyes et al. (1965) (Deffeyes et al., 1965) suggested that these strata are in their original depositional position, and were a slope facies, but this is difficult to support due to the lack of progradational geometries or any other related features, such as slumps and debrites.

Although, a tilted explanation is based on one outcrop in the Seroe Domi Formation, in this study we suggest there are two sub-units, a lower (aggradational platform) and upper unit (prograding platform), constituting the Seroe Domi Formation, as was also proposed for equivalent strata in the Bahamas by Vahrenkamp et al. (1991). The basal unit was affected by tectonic deformation soon after deposition, whereas the upper unit shows an irregular, mostly sigmoidal geometry that is driven by underlying topography and available accommodation space, with no deformation except slow vertical uplift. This sigmoidal geometry can be observed at the Seru Grandi locality (Figure 5) and represents platform edge to shallow upper slope facies of the quite steep margin of the modern Bonaire Island. In spite of the terrace morphology not being defined by the stratigraphy, it shows an important regional trend of progradation, as described by Alexander (1961 Fig. 10). The Upper Miocene platform prograded eastwards and pinches out below the Pleistocene deposits, which subsequently were buried to the east beneath the modern sediments of Lac Bai and Pekelmeer lagoon in the southeast of the island. The prograding platform has quite a complex structure as a result of the interaction between the original topography and the synsedimentary tectonic deformation during the Miocene (Hippolyte and Mann, 2011) and high-amplitude sea-level variations which can range from 60 to 100 m (Pomar, 1991). Finally, the Pleistocene platform with its flat-topped geometry pinches out towards the coastal areas separated from the previous platform by an erosional unconformity (Fig. 3).

The spatial distribution of dates suggests a trend of progressively younger carbonates towards the east/southeast as the platform prograded in this direction (Fig. 14). This trend is likely to be associated with regional tectonic effects that dominate the southern Caribbean

area. The resulting local tilting would have generated the topography that controlled the distribution of shallow-marine deposition.

7.1 Basement topography influencing bedding architecture

The basement is currently exposed in two main regions: in the northwest around the village of Rincon and in the eastern part of the island near Kralendijk (Figure 2). In the northwest, basement rocks give rise to 3 major topographic highs, with the rest of the volcanic exposure averaging around 40 m. One of the physiographic features is a conical hill with an elevation up to 130 m in the SW part of this basement region. The other two localities are linear parallel ridges from the NW to the center of that region. The maximum elevations for these ridges are 180 m and 130 m (Fig. 2). These ridges are directed SE towards the eastern volcanic region. Between the two volcanic regions are carbonate strata which have elevations between 70 and 140 m. The basement in the east is topographically lower, with a maximum elevation of about 70 m and an average of 25-30 m. Based on these observations, we infer that the island has been uplifted and tilted, causing shallow-water carbonate deposition to begin in the northwest and prograde east/southeast-wards.

During the geological evolution of Bonaire, the basement has been exposed and submerged on several occasions, allowing deposition on top of this sea-floor high. Evidence for this is provided by the remnant Cretaceous Rincon Limestone near Rincon Town (Hippolyte and Mann, 2011; Pijpers, 1933). This limestone was deposited during the Maastrichtian, a time of relatively high global sea-level (Bandoian and Murray, 1974; De Buisonjé, 1974; Hippolyte

and Mann, 2011; Pijpers, 1933). During the upper Eocene, fluvial conglomerate and sandstone of the Soebi Blanco Formation were deposited, a small section of which is exposed in the center of the island near Seru Largu and Santa Barbara (Zapata et al., 2014). These fluvial facies record uplift and erosion of the basement and the Rincon Limestone. During the Neogene, the island would have been relatively flat and marine transgression would have allowed dispersed coral communities to develop on the hard substrate, probably controlled by wave-energy levels and sea-level variations. The subsequent Middle to Late Miocene uplift of the volcanic basement mainly occurred in the western part of the island (Hippolyte and Mann, 2011). This created topography and the regional tilt to the east/southeast such that subsequent deposition filled the irregular accommodation space and progradational geometries developed towards the east/southeast. Finally, the younger, Pleistocene platform developed around the margin of the isolated platform during Quaternary sea-level highstands. The topography of Bonaire may well have been relatively stable from the Upper Miocene onwards, with only slow subsidence permitting Pleistocene highstands to be recorded around the island as reefal deposits.

8 Discussion

8.1 Allogenic controls on deposition

8.1.1 Wind and climate

The ITCZ regulates the rainfall over equatorial areas. Bonaire is at the present-time located north of the northern boundary of the ITCZ in a semi-arid weather band (Arbuszewski et al., 2013). However, Peterson and Haug (2006) suggested a more northward extent of the ITCZ during the Miocene. This process would have generated alternating wet and dry seasons.

However, the migration and impact of the ITCZ are poorly documented for the Miocene in the Caribbean region. Some models have been proposed for a shift in the ITCZ from the Pliocene to the present-day, based on data from an oceanographic expedition in the Cariaco Basin and computer-generated simulations (Chiang and Bitz, 2005; Peterson and Haug, 2006). Those models suggested the impact of the cold water influx on the ITCZ, which may have affected the carbonate factory during the Miocene. However, those models perhaps could be more applicable to the younger platform which was deposited in a similar climate regime to the present-day.

According to our results and published data (Lorscheid et al., 2017; Muhs et al., 2012; Obert et al., 2016), carbonate deposits on Bonaire record only 2 highstand stages, MIS5e and possibly MIS7-11, with warm and dry conditions which affected most of the Caribbean. On the other hand, Sibley (1982) suggested a wet-dry alternating climate for Bonaire based on dolomitization events. These observations may suggest a climate cyclicity which could have affected the diagenetic pathways of these deposits, especially for the first and second platforms which seem to have been strongly affected by dolomitization and meteoric diagenesis. This observation suggests that short-term climate cycles did not significantly affect the depositional pattern during the Miocene. However, sporadic high-energy events such as hurricane-like episodes may have caused fragmentation and reworking sediments represented by reworked red algal facies.

8.1.2 Caribbean Ocean circulation and nutrient supply

The first Miocene deposits (the aggradational platform) on Bonaire are dominated by corals and fragmented calcareous red algae which gradually became further enriched in red

algae as coral debris decreased in the coarse bioclastic facies. For the second, Upper Miocene-Pliocene platform (the prograding platform), environmental conditions may have restricted coral growth, but they provided a favorable setting for abundant red algae and large benthic foraminifera in relatively shallow waters. This evolution of facies during deposition of the aggradational platform suggests either a deepening-upward trend or an effect of increased nutrients. Nutrient supply to waters around Bonaire may have been controlled by continental runoff derived *via* the Orinoco River that flows north into the Caribbean Sea. During the Miocene this north-flowing marine current could have strengthened to bring dense water and an increased supply of nutrients through continental run off. However, uplift of the Andes in the Upper Miocene-Pliocene would have caused a shift in the drainage patterns farther to the east to the Orinoco's present-day position (Albert Villanueva, 2016; Hoorn et al., 1995). Although this scenario would have caused local nutrient enrichment, the shift from a coral-coralgal to a coralgal-large benthic foraminifera community has been reported from other localities in the region, such as the Cayman Islands and the Bahamas (McNeill et al., 1997; Reijmer et al., 2002), which are distant from the influence of the Orinoco.

An alternative scenario is that the dense, cold nutrient rich-water flowed from the South Atlantic to the Pacific as a result of open circulation through the Central American Seaway would have generated an environment hostile to the establishment of coral frameworks. In contrast, the young Pleistocene platform, which was deposited after 3.2 Ma (closure of Panama isthmus), shows a radical change to reef frameworks formed of head and branching corals (Haug and Tiedemann, 1998; Keigwin, 1982; Schneider and Schmittner,

2006; Tiedemann and Franz, 1997). This occurrence could be the result of increasing surface-water temperature and reducing nutrient supply, from the Pliocene onward, caused by the closure of the Central American Seaway (Gussone et al., 2004). In addition, the first appearance of the major reef-builders such *Acropora palmata* in the Caribbean area occurs at 3.6 Ma (McNeill et al., 1997), coincident with the development of modern reefs, as suggested by Pomar et al. (2017) for the Tethyan province (Figure 15). This event is consistent with the change of the style of carbonate sedimentation that we have documented here for Bonaire. Furthermore, the change in the geometries of the platforms, from prograding to flat-topped, also corresponds to the same events in the Bahamas (Reijmer et al., 2002) (Fig. 15).

8.1.3 Tectonics

Bonaire is close to the South Caribbean Plate Boundary Zone (SCPBZ), which has been experiencing transpression since the Miocene. This area of the Caribbean Plate is moving east relative to the South American Plate; it has an oblique component which has led to convergence and shallow subduction of the Caribbean Plate beneath the South American Plate to the south. The subduction is taking place north of Bonaire (known as the South Caribbean Deformation Belt, SCDB), and this has created an accretionary wedge among the sedimentary rocks within the SCPBZ because of tectonic uplift. Bonaire topography is partly a product of this tectonic uplift. However, as a result of this deformation there may also be subsidence taking place along the southern part of the island, in addition to the effect of platform progradation and sediment loading (Escalona and Mann, 2011; Gorney et al., 2007).

Based on the stratigraphic observations presented here, we suggest that deformation affected

the first, mid-Miocene platform (at Goto Meer) soon after deposition. This resulted in tilting of the mid-Miocene beds up to 30^{o}, the result of compressional stress associated with the South Caribbean Deformation Belt (SCDB), prior to the deposition of the next platform (Upper Miocene). After this event, basement topography was established and there was likely continued uplift in response to the compressional regime (Hippolyte and Mann, 2011).This deformation was indeed asymmetric and followed the major trend of the Caribbean plate movement to the east, reshaping the basement topography. During this period, the second prograding platform (Upper Miocene) was deposited and the accommodation space was controlled by basement topography and the general sea-level highstand, forcing the carbonates to prograde to the east. Younger platform strata on the northern side of Bonaire are uplifted approximately 8 m above sea level, whereas the same strata on the southern side of the island are buried due to basement subsidence beneath the modern lagoons of Pekelmeer and Lac Bai with their microbial-evaporitic carbonate deposits (Lucia, 1968; Sibley and Murray, 1972).

9 Summary and Conclusions

Interpretations of the interaction between stratigraphy and geomorphology on the island of Bonaire have been quite controversial and difficult to understand due to the complexity of this relationship. However, the results of this investigation reveal that the erosional terrace morphology is of less significance for the reconstruction of depositional events than previously reported. The internal stratigraphic architecture is clearly reflected in the dynamics of sedimentation episodes, in conjunction with allogenic controls, such as the major oceanographic and tectonic events in the region.

We defined three episodes in the evolution of the carbonate platforms: 1) An aggradational platform of Early-Middle Miocene age with well-bedded carbonates, showing a fining-upward trend from coarse mixed coral rudstone to medium-grained coralgal grain/pack-stone, partly dolomitized. 2) A progradational platform of Late Miocene-Pliocene age, which is formed of shallowing-upward prograding, offlapping units mainly composed of reworked red algal grain/packstone, with significant dolomitization. This succession passes upward and laterally into shoreline and aeolian deposits formed of coralgal grain/packstone and large benthic foraminifera grainstone and 3) The youngest platform (Pleistocene) with a reefal framework composed of a rich variety of coral-reef builders and bioclastic matrix. These platforms show a contrasting style and are separated by erosional unconformities, although they are only well-defined in key outcrops

Regional events, such as movements of the Caribbean plate relative to the South American plate and the closure of the Panamanian Isthmus, are dominant external controls on the contrasting style of the three carbonate depositional cycles. Caribbean tectonics deformed the first platform and shaped the topography of the basement which controlled sedimentation of the second platform. The style of deposition followed the regional tectonic trend in a predictable manner. Each platform is younger and located farther to the east (windward) relative to the previous one. In addition, the internal platform architecture shows sigmodal geometries from the eastward migration / progradation of the shelf break. Oceanographic conditions brought cold and nutrient-rich water on to the platform during the Miocene, but ocean currents and nutrient levels in the Caribbean changed after the closure of the Panamanian Isthmus, favoring the faunal turnover to reef-building organisms which

dominate the younger Neogene platform on Bonaire. This interpretation has significant implications for predicting isolated carbonate platform architecture in active tectonic settings, such as the Caribbean. If the regional tectonics are understood, geometries and facies distribution can be anticipated. Also, this study reveals the way isolated carbonate platforms respond to changes in ocean circulation and climate fluctuations, especially in the Caribbean. The results of this research also have implications for predicting carbonate facies and reservoir properties in areas of hydrocarbon exploration with a similar structural setting and platform styles.

10 Acknowledgements

We would like to thank Robet Widodo for assistance with field work and collaboration with sampling. In addition, we are grateful to CIEE Bonaire and especially Dr. Rita Peachey for all the help in the field. Furthermore, we would like to acknowledge Stinapa Bonaire, especially Paulo Bertuol for granting the research permission to sample inside the Washington Slagbaai National Park. Also, we are grateful to Dr. Steve Kazcmarek and Cameron Marche for XRD analysis at Western Michigan University. Furthermore we thank Dr. Youjun Deng for XRD measurements at Texas A&M University. We also would like to thank Dr. Ali Pourmand for assistance with U-Th dating in the Neptune Isotope Laboratory (NIL) at University of Miami. Finally, we would like to acknowledge Dan Hughes Company for provided funding for field work as a part of Jonathan Sulaica's Masters dissertation.

11 References

Albert Villanueva, E., 2016. Facies y secuencias deposicionales mixtas carbonático-siliciclásticas del mioceno inferior de la cuenca de Falcón (Noroeste de Venezuela) como

modelo exploratorio en el Caribe. PhD Dissertation University of Barcelona.

Alexander, C.S., 1961. The marine terraces of Aruba, Bonaire, and Curaçao, Netherlands Antilles. Annals of the Association of American Geographers 51, 102-123.

Arbuszewski, J.A., Cléroux, C., Bradtmiller, L., Mix, A., 2013. Meridional shifts of the Atlantic intertropical convergence zone since the Last Glacial Maximum. Nature Geoscience 6, 959-962.

Bak, R.P., 1977. Coral reefs and their zonation in Netherlands Antilles: modern and ancient reefs. AAPG Bulletin 4, 3-16.

Bandoian, C.A., Murray, R.C., 1974. Pliocene-pleistocene carbonate rocks of Bonaire, Netherlands Antilles. Geological Society of America Bulletin 85, 1243-1252.

Betzler, C., Eberli, G.P., Kroon, D., Wright, J.D., Swart, P.K., Nath, B.N., Alvarez-Zarikian, C.A., Alonso-García, M., Bialik, O.M., Blättler, C.L., 2016. The abrupt onset of the modern South Asian Monsoon winds. Scientific reports 6, srep29838.

Bosence, D., 2005. A genetic classification of carbonate platforms based on their basinal and tectonic settings in the Cenozoic. Sedimentary Geology 175, 49-72.

Bowling, R., Laya, J.C., Everett, M., in revision. Resolving Carbonate Platform Geometries on the Island of Bonaire, Caribbean Netherlands through Semi-Automatic GPR Facies Classification. Geophysical Journal International.

Braga, J.C., Martín, J.M., Aguirre, J., Baird, C.D., Grunnaleite, I., Jensen, N.B., Puga-Bernabéu, A., Sælen, G., Talbot, M.R., 2010. Middle-Miocene (Serravallian) temperate carbonates in a seaway connecting the Atlantic Ocean and the Mediterranean Sea (North

Betic Strait, S Spain). Sedimentary Geology 225, 19-33.

Budd, A.F., Petersen, R.A., McNeill, D.F., 1998. Stepwise faunal change during evolutionary turnover; a case study from the Neogene of Curacao, Netherlands Antilles. Palaios 13, 170-188.

Chiang, J.C., Bitz, C.M., 2005. Influence of high latitude ice cover on the marine Intertropical Convergence Zone. Climate Dynamics 25, 477-496.

Courgeon, S., Bourget, J., Jorry, S.J., 2016. A Pliocene–Quaternary analogue for ancient epeiric carbonate settings: The Malita intrashelf basin (Bonaparte Basin, northwest Australia). Aapg Bulletin 100, 565-595.

Courgeon, S., Jorry, S., Jouet, G., Camoin, G., BouDagher-Fadel, M., Bachèlery, P., Caline, B., Boichard, R., Révillon, S., Thomas, Y., 2017. Impact of tectonic and volcanism on the Neogene evolution of isolated carbonate platforms (SW Indian Ocean). Sedimentary Geology 355, 114-131.

De Buisonjé, P.H., 1963. Marine Terraces and Sub-aeric Sediments on the Netherlands Leeward Islands, Curaçao, Aruba and Bonaire, as Indications of Quaternary Changes in Sea Level and Climate: I, II. Geologisch Instituut, Universiteit van Amsterdam.

De Buisonjé, P.H., 1974. Neogene and quaternary geology of Aruba, Curaçao and Bonaire. PhD thesis, Universiteit van Amsterdam.

Deffeyes, K., Lucia, F.J., Weylt, P., 1964. Dolomitization: Observations on the Island of Bonaire, Netherlands Antittes. Science 143, 678-679.

Deffeyes, K.S., Lucia, F.J., Weyl, P.K., 1965. Dolomitization of Recent and Plio- Pleistocene

1 sediments by marine evaporite waters on Bonaire, Netherlands Antilles:, Dolomitization and
2 limestone Diagenesis. SEPM Special publication 13, pp. 71-88.

3 Della Porta, G., Kenter, J.A., Bahamonde, J.R., 2004. Depositional facies and stratal
4 geometry of an Upper Carboniferous prograding and aggrading high-relief carbonate
5 platform (Cantabrian Mountains, N Spain). Sedimentology 51, 267-295.

6 Dunham, R.J., 1962. Classification of carbonate rocks according to depositional texture.
7 AAPG Memoir Tulsa, pp. 108-121, 107 Pls.

8 Dustan, P., 1975. Growth and form in the reef-building coral Montastrea annularis. Marine
9 Biology 33, 101-107.

10 Eberli, G.P., Ginsburg, R.N., 1989. Cenozoic progradation of northwestern Great Bahama
11 Bank, a record of lateral platform growth and sea-level fluctuations, in: Crevello, P.D. (Ed.),
12 Controls on Carbonate Platforms and Basin Development. SEPM Special Publication 44, pp.
13 339-355.

14 Edwards, C.T., Saltzman, M.R., Leslie, S.A., Bergström, S.M., Sedlacek, A.R., Howard, A.,
15 Bauer, J.A., Sweet, W.C., Young, S.A., 2015. Strontium isotope ($^{87}Sr/^{86}Sr$) stratigraphy of
16 Ordovician bulk carbonate: Implications for preservation of primary seawater values. GSA
17 Bulletin 127, 1275-1289.

18 Embry, A.F., Klovan, J.E., 1971. A late Devonian reef tract on northeastern Banks Island,
19 NWT. Bulletin of Canadian Petroleum Geology 19, 730-781.

20 Engel, M., Brückner, H., Fürstenberg, S., Frenzel, P., Konopczak, A.M., Scheffers, A.,
21 Kelletat, D., May, S.M., Schäbitz, F., Daut, G., 2013. A prehistoric tsunami induced long-
22 lasting ecosystem changes on a semi-arid tropical island—the case of Boka Bartol (Bonaire,

Leeward Antilles). Naturwissenschaften 100, 51-67.

Escalona, A., Mann, P., 2011. Tectonics, basin subsidence mechanisms, and paleogeography of the Caribbean-South American plate boundary zone. Marine and Petroleum Geology 28, 8-39.

Felis, T., Giry, C., Scholz, D., Lohmann, G., Pfeiffer, M., Pätzold, J., Kölling, M., Scheffers, S.R., 2015. Tropical Atlantic temperature seasonality at the end of the last interglacial. Nature communications 6, 6159.

Fouke, B.W., Beets, C., Meyers, W.J., Hanson, G.N., Melillo, A.J., 1996. $^{87}Sr/^{86}Sr$ Chronostratigraphy and dolomitization history of the Seroe Domi Formation, Curaçao (Netherlands Antilles). Facies 35, 293-320.

Frébourg, G., Hasler, C.-A., Le Guern, P., Davaud, E., 2008. Facies characteristics and diversity in carbonate eolianites. Facies 54, 175-191.

Gorney, D., Escalona, A., Mann, P., Magnani, M.B., Group, B.S., 2007. Chronology of Cenozoic tectonic events in western Venezuela and the Leeward Antilles based on integration of offshore seismic reflection data and on-land geology. AAPG bulletin 91, 653-684.

Gussone, N., Eisenhauer, A., Tiedemann, R., Haug, G., Heuser, A., Bock, B., Nägler, T.F., Müller, A., 2004. Reconstruction of Caribbean sea surface temperature and salinity fluctuations in response to the Pliocene closure of the Central American Gateway and radiative forcing, using $\delta^{44/40}$ Ca, δ^{18} O and Mg/Ca ratios. Earth and Planetary Science Letters 227, 201-214.

Haug, G.H., Tiedemann, R., 1998. Effect of the formation of the Isthmus of Panama on

Atlantic Ocean thermohaline circulation. Nature 393, 673.

Herweijer, J., De Buisonjé, P., Zonneveld, J., 1977. Neogene and Quaternary geology and geomorphology. Guide to the field excursions on Curaçao, Bonaire and Aruba. STINAPA, 39-55.

Herweijer, J., Focke, J.W., 1978. Late Pleistocene depositional and denudational history of Aruba, Bonaire and Curagao (Netherlands Antilles). Geol. Mijnbouw 57, 177-187.

Hippolyte, J.-C., Mann, P., 2011. Neogene–Quaternary tectonic evolution of the Leeward Antilles islands (Aruba, Bonaire, Curaçao) from fault kinematic analysis. Marine and Petroleum Geology 28, 259-277.

Holbourn, A., Kuhnt, W., Kochhann, K.G., Andersen, N., Sebastian Meier, K., 2015. Global perturbation of the carbon cycle at the onset of the Miocene Climatic Optimum. Geology 43, 123-126.

Hoorn, C., Guerrero, J., Sarmiento, G.A., Lorente, M.A., 1995. Andean tectonics as a cause for changing drainage patterns in Miocene northern South America. Geology 23, 237-240.

Hornbach, M., Mann, P., Taylor, F., Bowen, S., 2010. Estimating the Age of Near-Shore Carbonate Slides Using Coral Reefs and Erosional Markers: A Case Study from Curaçao, Netherlands Antilles. The Sedimentary Record 8, 4-10.

Hu, C., Montgomery, E.T., Schmitt, R.W., Muller-Karger, F.E., 2004. The dispersal of the Amazon and Orinoco River water in the tropical Atlantic and Caribbean Sea: Observation from space and S-PALACE floats. Deep Sea Research Part II: Topical Studies in Oceanography 51, 1151-1171.

James, N., Wood, R., Dalrymple, R., James, N., 2010. Reefs and reef mounds. Facies Models 4, 421-447.

James, N.P., 1997. Cool-water carbonate depositional realm, in: James, N.P., Clarke, A.D. (Eds.), Cool-Water Carbonates. SEPM Special Publication 56, Tulsa, pp. 1-20.

James, N.P., Jones, B., 2015. Origin of Carbonate Rocks. John Wiley & Sons.

Jordan, T.H., 1975. The present-day motions of the Caribbean plate. Journal of Geophysical Research 80, 4433-4439.

Keigwin, L., 1982. Isotopic paleoceanography of the Caribbean and East Pacific: role of Panama uplift in late Neogene time. Science 217, 350-353.

Kenter, J.A., 1990. Carbonate platform flanks: slope angle and sediment fabric. Sedimentology 37, 777-794.

Kim, K.H., Lee, D.-J., 1999. Distribution and depositional environments of coralline lithofacies in uplifted Pleistocene coral reefs of Bonaire, Netherlands Antilles. Journal of Paleontology Society of Korean 15, 115-133.

Laya, J.C., Whitaker, F., Teoh, C.P., Tucker, M.E., Gabellone, T., Marche, C., Kaczmarek, S., 2017. Spatial Distribution of dolomitization within a complex stratigraphy in an isolated carbonate platform, Bonaire, Netherlands Antilles, IAS Meeting IAS, Toulouse, France.

Lisiecki, L.E., Raymo, M.E., 2005. A Pliocene-Pleistocene stack of 57 globally distributed benthic $\delta^{18}O$ records. Paleoceanography 20.

Lorscheid, T., Felis, T., Stocchi, P., Obert, J.C., Scholz, D., Rovere, A., 2017. Tides in the

Last Interglacial: insights from notch geometry and palaeo tidal models in Bonaire, Netherland Antilles. Scientific reports 7, 16241.

Lucia, F., 1968. Recent sediments and diagenesis of south Bonaire, Netherlands Antilles. Journal of Sedimentary Research 38, 845-858.

Martis, A., van Oldenborgh, G.J., Burgers, G., 2002. Predicting rainfall in the Dutch Caribbean—more than El Nino? International Journal of Climatology 22, 1219-1234.

Matthews, R., 1968. Carbonate diagenesis: equilibration of sedimentary mineralogy to the subaerial environment; coral cap of Barbados, West Indies. Journal of Sedimentary Research 38, 1110-1119.

McArthur, J., Howarth, R., Shields, G., 2012. Strontium isotope stratigraphy, The geologic time scale. Elsevier, pp. 127-144.

McNeill, D.F., Budd, A.F., Borne, P.F., 1997. Earlier (late Pliocene) first appearance of the Caribbean reef-building coral Acropora palmata: Stratigraphic and evolutionary implications. Geology 25, 891-894.

McNeill, D.F., Klaus, J.S., Budd, A.F., Lutz, B.P., Ishman, S.E., 2012. Late Neogene chronology and sequence stratigraphy of mixed carbonate-siliciclastic deposits of the Cibao Basin, Dominican Republic. GSA Bulletin 124, 35-58.

Milliman, J., 1974. Marine carbonates, recent sedimentary carbonates, 1. Springer-Verlag, Berlin.

Muhs, D.R., Pandolfi, J.M., Simmons, K.R., Schumann, R.R., 2012. Sea-level history of past interglacial periods from uranium-series dating of corals, Curaçao, Leeward Antilles islands.

Quaternary Research 78, 157-169.

Nisancioglu, K.H., Raymo, M.E., Stone, P.H., 2003. Reorganization of Miocene deep water circulation in response to the shoaling of the Central American Seaway. Paleoceanography 18, 1006.

Obert, J.C., Scholz, D., Felis, T., Brocas, W.M., Jochum, K.P., Andreae, M.O., 2016. ^{230}Th/U dating of Last Interglacial brain corals from Bonaire (southern Caribbean) using bulk and theca wall material. Geochimica et Cosmochimica Acta 178, 20-40.

Pandolfi, J.M., Jackson, J.B., 2001. Community structure of Pleistocene coral reefs of Curaçao, Netherlands Antilles. Ecological monographs 71, 49-67.

Pedoja, K., Husson, L., Johnson, M.E., Melnick, D., Witt, C., Pochat, S., Nexer, M., Delcaillau, B., Pinegina, T., Poprawski, Y., 2014. Coastal staircase sequences reflecting sea-level oscillations and tectonic uplift during the Quaternary and Neogene. Earth-Science Reviews 132, 13-38.

Pérez, O.J., Bilham, R., Bendick, R., Velandia, J.R., Hernández, N., Moncayo, C., Hoyer, M., Kozuch, M., 2001. Velocity field across the southern Caribbean plate boundary and estimates of Caribbean/South-American plate motion using GPS geodesy 1994–2000. Geophysical Research Letters 28, 2987-2990.

Peterson, L.C., Haug, G.H., 2006. Variability in the mean latitude of the Atlantic Intertropical Convergence Zone as recorded by riverine input of sediments to the Cariaco Basin (Venezuela). Palaeogeography, Palaeoclimatology, Palaeoecology 234, 97-113.

Pijpers, P.J., 1933. Geology and paleontology of Bonaire (DWI). PhD Dissertation Utrecht, Netherlands.

Pindell, J.L., Cande, S., Pitman III, W.C., Rowley, D.B., Dewey, J.F., LaBrecque, J., Haxby, W., 1988. A plate-kinematic framework for models of Caribbean evolution. Tectonophysics 155, 121-138.

Pomar, L., 1991. Reef geometries, erosion surfaces and high-frequency sea-level changes, upper Miocene Reef Complex, Mallorca, Spain. Sedimentology 38, 243-269.

Pomar, L., 2001. Types of carbonate platforms: a genetic approach. Basin Research 13, 313-334.

Pomar, L., Baceta, J.I., Hallock, P., Mateu-Vicens, G., Basso, D., 2017. Reef building and carbonate production modes in the west-central Tethys during the Cenozoic. Marine and Petroleum Geology 83, 261-304.

Pomar, L., Bassant, P., Brandano, M., Ruchonnet, C., Janson, X., 2012. Impact of carbonate producing biota on platform architecture: insights from Miocene examples of the Mediterranean region. Earth-Science Reviews 113, 186-211.

Pomar, L., Esteban, M., Martinez, W., Espino, D., de Ott, V.C., Benkovics, L., Leyva, T.C., 2015. Oligocene–Miocene carbonates of the Perla Field, Offshore Venezuela: Depositional model and facies architecture, in: Bartollini, C., Mann, P. (Eds.), Petroleum Geology and Potential of the Colombian Caribbean Margin. AAPG Memoir 108, pp. 647-673.

Pomar, L., Hallock, P., 2008. Carbonate factories: a conundrum in sedimentary geology. Earth-Science Reviews 87, 134-169.

Pomar, L., Kendall, C., 2008. Architecture of carbonate platforms: a response to hydrodynamics and evolving ecology, Controls on carbonate platform and reef development. SEPM Special Publication, pp. 187-216.

Purser, B., Bosence, D., 1998. Organization and scientific contributions in sedimentation and tectonics of rift basins: Red Sea-Gulf of Aden, Sedimentation and Tectonics in Rift Basins Red Sea:-Gulf of Aden. Springer, pp. 3-8.

Reijmer, J.J., Betzler, C., Kroon, D., Tiedemann, R., Eberli, G.P., 2002. Bahamian carbonate platform development in response to sea-level changes and the closure of the Isthmus of Panama. International Journal of Earth Sciences 91, 482-489.

Rixhon, G., May, S.M., Engel, M., Mechernich, S., Schroeder-Ritzrau, A., Frank, N., Fohlmeister, J., Boulvain, F., Dunai, T., Brückner, H., 2018. Multiple dating approach (^{14}C, ^{23}0Th/U and ^{36}Cl) of tsunami-transported reef-top boulders on Bonaire (Leeward Antilles)–Current achievements and challenges. Marine Geology 396, 100-113.

Ryan, W.B., Carbotte, S.M., Coplan, J.O., O'Hara, S., Melkonian, A., Arko, R., Weissel, R.A., Ferrini, V., Goodwillie, A., Nitsche, F., 2009. Global multi-resolution topography synthesis. Geochemistry, Geophysics, Geosystems 10.

Schellmann, G., Radtke, U., Scheffers, A., Whelan, F., Kelletat, D., 2004. ESR dating of coral reef terraces on Curaçao (Netherlands Antilles) with estimates of younger Pleistocene sea level elevations. Journal of Coastal Research, 947-957.

Schlager, W., 2003. Benthic carbonate factories of the Phanerozoic. International Journal of Earth Sciences 92, 445-464.

Schlager, W., Reijmer, J.J., Droxler, A., 1994. Highstand shedding of carbonate platforms. Journal of Sedimentary Research 64.

Schneider, B., Schmittner, A., 2006. Simulating the impact of the Panamanian seaway closure on ocean circulation, marine productivity and nutrient cycling. Earth and Planetary

Science Letters 246, 367-380.

Sibley, D.F., 1980. Climatic control of dolomitization, Seroe Domi Formation (Pliocene), Bonaire, N.A., in: Zenger, D.H., Dunham, J.B., Ethington, R.L. (Eds.), Concepts and Models of Dolomitization. SEPM Speacial Publication 28, pp. 247-258,.

Sibley, D.F., 1982. The origin of common dolomite fabrics: clues from the Pliocene. Journal of Sedimentary Research 52, 1087-1100.

Sibley, D.F., Murray, R.C., 1972. Marine diagenesis of carbonate sediment, Bonaire, Netherlands Antilles. Journal of Sedimentary Research 42, 168-178.

Stehli, F.G., Wells, J.W., 1971. Diversity and age patterns in hermatypic corals. Systematic Zoology 20, 115-126.

Sulaica, J.L., 2015. Facies Distribution and Paleogeographic Evolution of Pleistocene Carbonates in Bonaire, Netherlands Antilles. Texas A&M University

Thompson, P., Kempton, P., White, R., Saunders, A., Kerr, A.C., Tarney, J., Pringle, M., 2004. Elemental, Hf–Nd isotopic and geochronological constraints on an island arc sequence associated with the Cretaceous Caribbean plateau: Bonaire, Dutch Antilles. Lithos 74, 91-116.

Tiedemann, R., Franz, S., 1997. 20. Deep-water circulation, chemistry, and terrigenous sediment supply in the equatorial Atlantic during the Pliocene, 3.3-2.6 Ma and 5-4.5 Ma, Proc. Ocean Drill. Program, Sci. Results, pp. 299-318.

Trenkamp, R., Kellogg, J.N., Freymueller, J.T., Mora, H.P., 2002. Wide plate margin deformation, southern Central America and northwestern South America, CASA GPS

observations. Journal of South American Earth Sciences 15, 157-171.

Vahrenkamp, V.C., Swart, P.K., Ruiz, J., 1991. Episodic dolomitization of late Cenozoic carbonates in the Bahamas; evidence from strontium isotopes. Journal of Sedimentary Research 61, 1002-1014.

Van Der Lelij, R., Spikings, R.A., Kerr, A.C., Kounov, A., Cosca, M., Chew, D., Villagomez, D., 2010. Thermochronology and tectonics of the Leeward Antilles: Evolution of the southern Caribbean Plate boundary zone. Tectonics 29, 1-30.

van Duyl, F., 1985. Atlas of the living reefs of Curaçao and Bonaire (Netherlands Antilles). Utrecht, Natuurwetenschappelijke studiekring voor Suriname en de Nederlandse Antillen, 117, 35 p.

Waelbroeck, C., Labeyrie, L., Michel, E., Duplessy, J.C., McManus, J., Lambeck, K., Balbon, E., Labracherie, M., 2002. Sea-level and deep water temperature changes derived from benthic foraminifera isotopic records. Quaternary Science Reviews 21, 295-305.

Wells, J.W., 1957. Corals. Geological Society of America Memoirs 67, 1087-1104.

Wilson, M., Vecsei, A., 2005. The apparent paradox of abundant foramol facies in low latitudes: their environmental significance and effect on platform development. Earth-Science Reviews 69, 133-168.

Zapata, S., Cardona, A., Montes, C., Valencia, V., Vervoort, J., Reiners, P., 2014. Provenance of the Eocene soebi blanco formation, Bonaire, Leeward Antilles: Correlations with post-Eocene tectonic evolution of northern South America. Journal of South American Earth Sciences 52, 179-193.

1

12 Figure captions

Figure 1. A) Digital relief image of Caribbean Sea and B) three-dimensional projection of the ABC island showing the location of the main areas of study. Modified from Ryan et al. (2009), also available at http://www.geomapapp.org.

Figure 2: Geological map and stratigraphic column for Bonaire. Rectangles are study areas and ovals are major population centers. Modified from Hippolyte and Mann (2011).

Figure 3: W-E schematic profile diagram showing the relationship of the three platforms episodes on Bonaire. Triangle indicates mean sea level (MSL).

Figure 4: Stratal architecture and plane polarized light (PPL) thin-section photomicrographs of samples of the Mid-Miocene aggradational platform at Goto Meer, NW Bonaire. Blue is epoxy resin showing porosity. A) Interpreted Stratal architecture of the Mid-Miocene aggradational platform. B) Mixed coral rudstone grainstone facies (outlined) mixed with small fraction of foraminifera and shell fragments. C) Coralgal facies consisting of red algae, echinoderms, shell fragments and coral grains.

Figure 5: Seru Grandi outcrop showing the architecture of the prograding platform stage (Upper Miocene-Pliocene) and bioclast component distribution in the strata. Red bar represents the core sample location which shows the transition between underlying prograding platform stage and the overlying flat-topped platform stage (Figure 6).

Figure 6: Plane polarized light images of thin sections and core sample of subfacies associated with prograding platform stage. Blue is epoxy resin showing porosity. A) Coralgal

grainstone and packstone facies with abundant red algae (RA) fragments. B) Encrusting red algae (ERA) rich grainstone/packstone. C) Mimetic and partially fabric destructive dolomitized facies associated with red algae –rich packstone. D) Reworked red algal (RA) E) Core sample of the transition between underlying prograding platform stage and the overlying flat-topped platform stage. F) Coral fragments encrusted by red algae and reworked bioclastic material. grainstone/packestone. G) Unconformity/transition shown as darker material in upper left half of thin section, bordered by coralline red algae crust from the the underlying red algae rich prograding platform facies. H) Dolomitized red algal-rich facies characterized by mimetic structure and moldic porosity.

Figure 7: A) Aeolinite deposits with large scale cross stratification. Panoramic view of Seru Largu outcrop. White spots showing porosity. Note person for scale (circled). B) Schematic interpretation of the internal stratigraphic architecture. C) Thin section photomicrograph of dominant facies for this deposit comprising Large Benthic Foraminifera (LBF) and Red Algae (RA) grainstone main facies for this deposit. D) Zoomed-in view of C), highlighting skeletal composition of the aeolinite deposits.

Figure 8: Field photo and schematic interpretation of Boka Chikitu outcrop. A) Reefal deposits showing flat-topped geometries, formed primarily of *Monstastrea sp*., of the Pleistocene flat-topped platform stage from Boca Chikitu. Arrow with ages of *Monstastrea sp.* heads acquired from U-Th dating. Seru Grandi (Figure 5) in background. B) Schematic interpretation of *Monstastrea sp*. amongst grainstones.

Figure 9: Plane polarized light images of thin sections (Blue is epoxy resin showing porosity)

from Bolivia and an outcrop photo from Tolo. A) *Montastrea sp*. fragment showing well-defined internal structure. Note the contact between the coral fragment and bioclastic matrix (white arrow). B) Acropora cervicornis Floatstone. Note the reddish branching structures (arrows). C) Gastropod-green algae grainstone/packstone. D) Coralgal Grainstone/Packestone.

Figure 10: Coral-rich boulders mainly formed of *Montastrea sp., Acropora palmata* and *Porites sp.* with encrusted coralline algae deposits. (A) encrustations can reach 10's of centimeter thick between boulders. (B) Close-up of coral boulder and red algae crust.

Figure 11. $^{87}Sr/^{86}Sr$ ratios curve of the three major facies. Age model for $^{87}Sr/^{86}Sr$ ratios based on McArthur et al. (2012). Red dots represent samples with more than 60% dolomite, blue dots represent samples with less than 60% dolomite.

Figure 12: Schematic depositional environment diagram for the progradational (Upper Miocene-Pliocene) platforms.

Figure 13: Schematic reefal facies distribution pattern for the flat-topped reefal (Pleistocene) platforms.

Figure 14: Map showing the distribution of platforms based on facies and Sr isotope dating ages, showing the broad-scale progradational pattern of Neogene carbonate deposition (blue arrows).

Figure 15: Chart of depositional, oceanographic and tectonic events that have contributed to the stratigraphic architecture of Bonaire. Green horizontal shades represent main environmental events which are concurrent with platform boundaries.

Table 1: Carbonate facies descriptions with interpretations of depositional environment

Platform	Facies	Brief description	Interpretation
Aggrading platform deposits (Lower-Middle Miocene)	*Mixed-coral rudstone/grainstone*	Large fragments of coral (*Montastrea* and *Porites* sp.) encrusted by thin *Neogoniolithon sp.* Intergranular cavities filled with fragments of green algae, echinoids, red algae and minor planktonic foraminifera.	High-energy, shallow-marine environment from presence of broken fragments of *Monstastrea* which indicate less than 10 m water depth. No corals in living position so likely fragments transported few meters from forereef. Planktonic foraminifera suggest open-marine conditions. Some reworked volcanic rock fragments.
	Coralgal grainstone/packstone	Grainstone /packstone comprised mainly of red algae and few coral fragments. Broken and abraded branches of *Lithothamnion* sp common, in addition, angular–rounded coral fragments (*Porites* sp., *Montastrea* sp.). Some bioclasts partially dissolved. Large benthic foraminifera (*Amphistegina* sp.) occur sporadically; rare brachiopod, echinoid and gastropod fragments. This facies mostly calcitic, locally dolomitized.	High-energy environment. Coralline red algae abundant; limited coral fragments indicate slightly deeper and cooler conditions. Increasing amount of large benthic foraminifera and finer-grained bioclasts suggest reworking by waves and currents moving away from reef front.
Progradational platform deposits (Upper Miocene-Pliocene)	*Coralgal grainstone/packstone*	Fine to medium-grained bioclast fragments of red algae (*Spongites* sp. *and Lithothamnion* sp), corals (*Acropora* sp., *Porites* sp., *Montastrea* sp), echinoids, bivalves, gastropods and large benthic foraminifera (*Amphistegina sp.)*. Most grains coated by micrite, probably a microbialite crust. This facies is calcitic with locally bladed and drusy cements. Some fine-sand brownish volcaniclastic fragments.	High-energy conditions dominated. Coralline red algae abundant and limited coral fragments indicate slightly deeper and cooler conditions. Increasing large benthic foraminifera content and fine-grained skeletal component suggest reworking by waves and currents moving away from the platform margin.
	Encrusting red algal-rich and rhodolite grainstone/packstone	Facies dominated by different taxa of encrusting coralline red algae including *Sporolithon* sp., *Spongites* sp., *Lithothamnion* sp., and *Neogoniolithon* sp., as well as encrusting foraminifera and large benthic foraminifera which are commonly dissolved out. This facies partly to completely dolomitized in mimetic, non-mimetic and sucrosic textures. Dolomite cements with zoned crystal habit and cloudy centres as well as clean crystal rhombs.	Although red algae can live in slightly deeper water, combination with large benthic foraminifera and possible hard substrates suggest shallow-marine upper platform within the upper photic zone with low-moderate energy at 0-30 m depth.
	Reworked red algal-rich grainstone/packstone	Variety of calcareous algae with high degree of fragmentation, abrasion and micritization. Skeletal grains mostly well-sorted and subrounded to rounded; some angular. This facies partly to completely dolomitized with microcrystalline dolomite cements and replacement dolomite within the algal internal structure. Bladed and drusy calcite also present.	High degree of fragmentation and abrasion indicate high-energy setting. Low diversity of bioclasts and abundant red algae suggest sediment supplied from shallow shelf.

	Large benthic foraminifera grainstone	Fine-grained, well-sorted grainstone with abundant large benthic foraminifera *Amphistegina sp.* Also, *Cycloclypeus* and Miogypsinids present. Brachiopod fragments common and rounded peloids. This facies is mostly calcitic with no evidence of dolomite cementation or replacement. High-angle cross-stratification common as well as limited low-angle planar cross-bedding.	High-energy environments, driven by coastal and aeolian processes. Shoreline sand-body of shoreface-foreshore-aeolian backshore facies.
Flat-topped Reefal platform deposits (Pleistocene)	*Montastrea-rich boundstone*	Mostly comprised of *Montastrea annularis* in living position mixed with other species such as *Montastrea cavernosa* and *Diploria strigose*, *Diploria clivosa*, *Acropora palmata* and *Porites* sp. They grow vertically and spread out, and can exceed 3 m in height. Internal cavities are filled with medium-grained bioclastic grainstone formed of green algae, gastropods and echinoids.	*Montastrea annularis* typical of low to medium-energy waters. This facies likely deposited in a lagoonal environment, protected by a barrier of branched corals from open sea. Coral boundstone represents reef core to back reef.
	Acropora cervicornis floatstone	Composed of *Acropora cervicornis,* with small amounts of *Diploria sp. Acropora cervicornis* is partially to completely dissolved out. Rubble of *A. cervicornis* branches. Wackestone - packstone texture surrounding coral branches formed of planktonic foraminifera and echinoids. This facies is calcitic with clear calcite drusy cements.	*Acropora cervicornis* requires decreased amounts of wave energy to thrive. Typical of reef front as in modern reefs, at depths between 4-12 m. Abundant fragments from damage by periodic storm waves.
	Montastrea-rich rudstone	Coral-rich boulders of *Montastrea*, *Acropora* p*almata* and *Porites* sp. with coralline algal encrustations which may reach 10s cm thick.	The dynamic of deposition is interpreted as storm events with enough energy to reworked significant volume of reef derived material in the windward side of the island. Subsequently, those broken boulders may have been flooded and coralline red algae developed a thick crust in individual fragment.
	Gastropod-green algal grainstone/packstone	Characterized by bioclasts of gastropods, green algae (*Halimeda* sp.), minor red algae and foraminifera. Dissolution of aragonitic skeletons common. Microcrystalline calcite cements common.	Photozoan aragonitic material common suggesting shallow-marine, coastal to platform interior deposits. This facies also filling cavities between reef-building organisms.

Coralgal grainstone/packstone	Composed of fine-grained bioclasts of red algae (*Corallinacea*), coral (*Acropora sp.*), calcareous green algae, bivalves, gastropods, bryozoans and foraminifera (*Amphistegina sp.)*. Most abundant bioclasts are coral and coralline red algae, which non-crustose and articulated. Some fine-grained volcaniclastic material present.	High-energy environment dominated by coralline red algae and limited coral indicating slightly deeper and cooler conditions. Increasing amount of large benthic foraminifera and finer grained skeletal debris suggest reworking by waves and currents moving away from the platform margin.

Table 2: Mineralogical and geochemical data for three platform episodes from a range of locations (shown on Figure 1). $^{87}Sr/^{86}Sr$ dates are based on age model of McArthur et al (2012).

Platforms	Location	Sample	$\delta^{13}C$	$\delta^{18}O$	Sr Isotope Average	% Dolomite	% Calcite	% Aragonite	Fe (ppm)	Mn (ppm)	Al (ppm)	Sr (ppm)	Sr Age Model (Ma)	U-Th Dates (Ky)
Aggadational	Goto Meer	25_13	**-4.27**	**-1.85**	0.7083274	**0.00%**	**100.00%**	**0.00%**	1098.1	482.5	1224.1	135.9	21.7	
	Goto Meer	25_5	**-4.63**	**-2.85**	0.7084912	**0.00%**	**100.00%**	**0.00%**	825.2	128.8	1013.7	80.6	18.9	
	Goto Meer	25_12	**-4.88**	**-2.21**	0.7085727	**0.00%**	**100.00%**	**0.00%**	1374.8	305.2	864.8	111.4	18	
	Goto Meer	25_10	**0.71**	**2.65**	0.7089885	**92.51%**	**7.49%**	**0.00%**	3053.0	665.5	185.4	197.4	6	
Progradational	Bolivia	20BON1	**1.35**	**2.48**	0.7087244	**86.64%**	**13.36%**	**0.00%**	148.7	24.9	0.0	168.5	16	
	Seru Grandi	27_5_1	**1.67**	**1.62**	0.7088418	**68.81%**	**31.19%**	**0.00%**	1133.2	119.5	493.8	217.4	11.6	
	Bolivia	15_3_1	**2.08**	**3.06**	0.7088991	**93.81%**	**6.19%**	**0.00%**	130.9	12.2	0.0	136.1	9.5	
	Seru Grandi	14_5_1	**-4.46**	**-2.13**	0.7088995	**19.00%**	**81.00%**	**0.00%**	886.7	65.4	625.6	233.3	9.4	
	Bike Trail	19BON4	**-1.24**	**-1.36**	0.7089152	**65.53%**	**34.47%**	**0.00%**	205.0	34.5	498.2	179.8	9	
	Bike Trail	19BON5	**0.91**	**2.55**	0.7089172	**92.48%**	**7.52%**	**0.00%**	345.1	22.8	0.0	149.3	8.9	
	Seru Largu	16BON1	**-6.48**	**-4.75**	0.7089273	**0.00%**	**100.00%**	**0.00%**	279.9	24.2	606.0	705.7	8	
	Bike Trail	19BON7	**-1.06**	**-1.46**	0.7089381	**66.61%**	**33.39%**	**0.00%**	23.8	13.8	0.0	131.3	7.9	
	Seru Grandi	Line 1_SG 14	**3.06**	**3.49**	0.7089415	**98.72%**	**1.28%**	**0.00%**	359.5	42.8	231.0	118.5	7.7	
	Seru Grandi	13_4_1	**3.33**	**4.03**	0.7089438	**98.54%**	**1.46%**	**0.00%**	581.3	22.8	314.5	618.7	7.5	
	Seru Grandi	26_6_4	**3.19**	**3.82**	0.7089465	**76.56%**	**23.44%**	**0.00%**	130.2	41.3	0.0	148.6	7.2	
	Bike Trail	4BON3	**-3.54**	**-0.10**	0.7089468	**55.16%**	**44.84%**	**0.00%**	78.2	5.8	0.0	150.3	7.1	
	Seru Grandi	13_2_1	**3.42**	**4.04**	0.7089479	**97.63%**	**2.37%**	**0.00%**	4176.4	122.6	0.0	219.3	6.9	
	Santa Barbara	20BON2	**0.90**	**2.39**	0.7089579	**96.04%**	**3.96%**	**0.00%**	115.1	45.2	0.0	163.8	6.8	
	Seru Grandi	Line 1_SG 16	**3.42**	**4.23**	0.7089671	**98.98%**	**1.02%**	**0.00%**	232.6	36.6	255.8	109.0	6.7	
	Seru Grandi	Line 1_SG 15	**3.34**	**3.96**	0.7089734	**99.16%**	**0.84%**	**0.00%**	402.3	45.5	332.7	142.7	6.6	
	Seru Grandi	14_7_1	**0.99**	**2.42**	0.7089743	**73.45%**	**26.55%**	**0.00%**	287.2	40.6	0.0	152.4	6.4	
	Bike Trail	19BON9	**0.49**	**2.15**	0.7089786	**90.59%**	**9.41%**	**0.00%**	58.5	8.9	0.0	160.8	6.3	
	Seru Grandi	14_2_1	**3.43**	**3.87**	0.7089787	**98.32%**	**1.68%**	**0.00%**	144.5	39.1	68.9	217.6	6.2	

	Seru Grandi	Line 2_SG 10	**3.36**	**4.23**	0.7089848	**98.96%**	**1.04%**	**0.00%**	175.7	22.9	157.4	105.2	6.1	
	Seru Grandi	15BON1	**0.80**	**2.17**	0.7089921	**73.12%**	**26.88%**	**0.00%**	270.5	38.3	0.0	145.1	6.05	
	Seru Grandi	27_9_1	**2.99**	**4.07**	0.7089990	**98.61%**	**1.39%**	**0.00%**	236.8	46.3	0.0	217.6	5.9	
	Seru Grandi	Line 1 Wdg 1_1	**-2.80**	**-3.15**	0.7090052	**0.40%**	**57.92%**	**41.68%**	105.8	27.7	119.0	496.2	5.7	
	Seru Grandi	27_8_1	**3.25**	**3.99**	0.7090074	**97.56%**	**2.44%**	**0.00%**	2887.9	47.7	0.0	153.3	5.5	
	Rincon south	13_8_1			0.7090079	**90.44%**	**9.56%**	**0.00%**	105.8	35.5	0.0	167.6	5.5	
	Seru Grandi	27_1_1	**2.96**	**3.81**	0.7090122	**99.00%**	**1.00%**	**0.00%**	373.0	51.7	0.0	180.3	5.4	
	Seru Grandi	15BON3	**2.33**	**2.86**	0.7090348	**92.87%**	**7.13%**	**0.00%**	601.9	92.4	577.9	362.0	4.9	
	Bike Trail	15_1_1	**-7.45**	**-4.90**	0.7090351	**0.00%**	**100.00%**	**0.00%**	135.0	17.0	0.0	355.5	4.8	
	Bike Trail	19BON8	**-0.78**	**1.34**	0.7090380	**81.53%**	**18.47%**	**0.00%**	174.0	11.5	0.0	89.4	4.7	
Flat-Topped Platform	Lagun	8_3_2	**-5.69**	**-4.52**	0.7090672	**0.00%**	**100.00%**	**0.00%**	63.4	13.1	29.2	1410.7	2.4	
	Boka Onima	26_8_7	**-5.03**	**-3.50**	0.7090900	**0.00%**	**100.00%**	**0.00%**	728.6	71.3	483.5	202.5	2	
	Tolo	9_2_4	**-6.67**	**-3.83**	0.7090909	**0.00%**	**100.00%**	**0.00%**	67.5	27.5	0.0	318.6	1.9	
	Bolivia	12_2_2	**-5.82**	**-4.70**	0.7090922	**0.00%**	**100.00%**	**0.00%**	77.8	14.8	0.0	1092.1	1.8	
	Bolivia	12_2_1	**-4.45**	**-4.15**	0.7090923	**0.00%**	**100.00%**	**0.00%**	14.5	6.6	0.0	484.7	1.7	
	Boka Onima	26_8_2	**-6.91**	**-3.91**	0.7091012	**0.00%**	**100.00%**	**0.00%**	1257.7	59.6	1289.5	344.0	1.6	
	Boka Onima	26_8_5	**-6.17**	**-3.49**	0.7091014	**0.00%**	**100.00%**	**0.00%**	1008.7	63.0	662.7	201.1	1.5	
	Tolo	9_2_1	**-3.80**	**-3.67**	0.7091027	**0.00%**	**100.00%**	**0.00%**	24.1	24.2	0.0	247.6	1.5	
	Bolivia	12_6_1	**-2.58**	**-2.32**	0.7091043	**0.00%**	**29.98%**	**70.02%**	78.0	16.8	62.8	3245.5	1.45	
	Seru Grandi	14_3_1	**-3.26**	**-3.94**	0.7091216	**0.00%**	**100.00%**	**0.00%**					1.2	
	Boka Onima	26_8_4	**-6.66**	**-3.69**	0.7091299	**0.00%**	**100.00%**	**0.00%**	187.1	25.9	164.4	814.7	1	
	Lagun	8_3_1	**-10.64**	**-4.89**	0.7091387	**0.00%**	**100.00%**	**0.00%**	607.2	106.2	784.7	89.4	0.8	
	Boka Onima	26_7_1	**-0.20**	**-3.14**	0.7092270	**0.00%**	**0.99%**	**99.01%**	54.2	9.0	34.7	7073.9	0.1	115.1 ± 1.0

Boka Onima	26_7_2										133.0 ± 1.4
Bolivia	12_1_1			**0.00%**	**100.00%**	**0.00%**	262.0	9.7	0.0	1764.9	715.6 ± 430
Bolivia	12_7_1	**-0.21**	**-1.88**	**0.00%**	**20.59%**	**79.41%**	0.0	9.0	0.0	2883.6	124.9 ± 0.9
Bolivia	12_8_1	**-0.62**	**-3.86**	**0.00%**	**0.23%**	**99.77%**	0.0	2.0	0.0	6756.7	131.7 ± 1.5
Bolivia	12_8_2	**-0.25**	**-1.88**				64.7	6.3	0.0	2231.6	198.9 ± 1.2
Seru Grandi	27_2_1	**0.13**	**-2.89**	**0.36%**	**21.81%**	**77.83%**	31.6	4.2	0.0	5767.2	127.0 ± 1.3
Seru Grandi	13_1_1	**-4.93**	**-2.04**	**0.00%**	**39.28%**	**60.72%**	860.9	24.0	453.8	2563.5	124.4± 1.3
Boca Onima	Boca Sample 5										127.1 ± 1.2

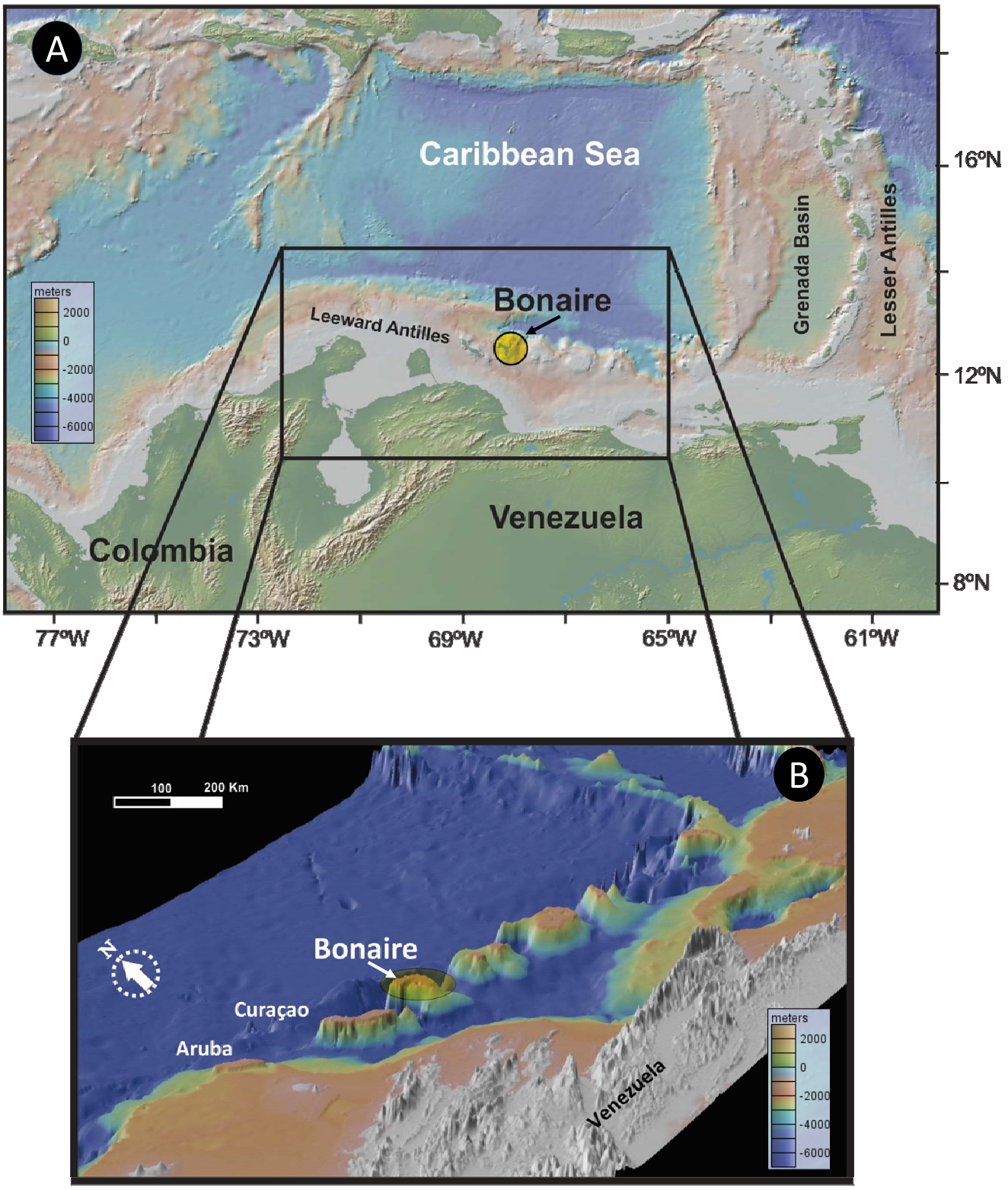

Figure 1. A) Digital relief image of Caribbean Sea and B) three-dimensional projection of the ABC island showing the location of the main areas of study. Modified from Ryan et al. (2009), also available at http://www.geomapapp.org.

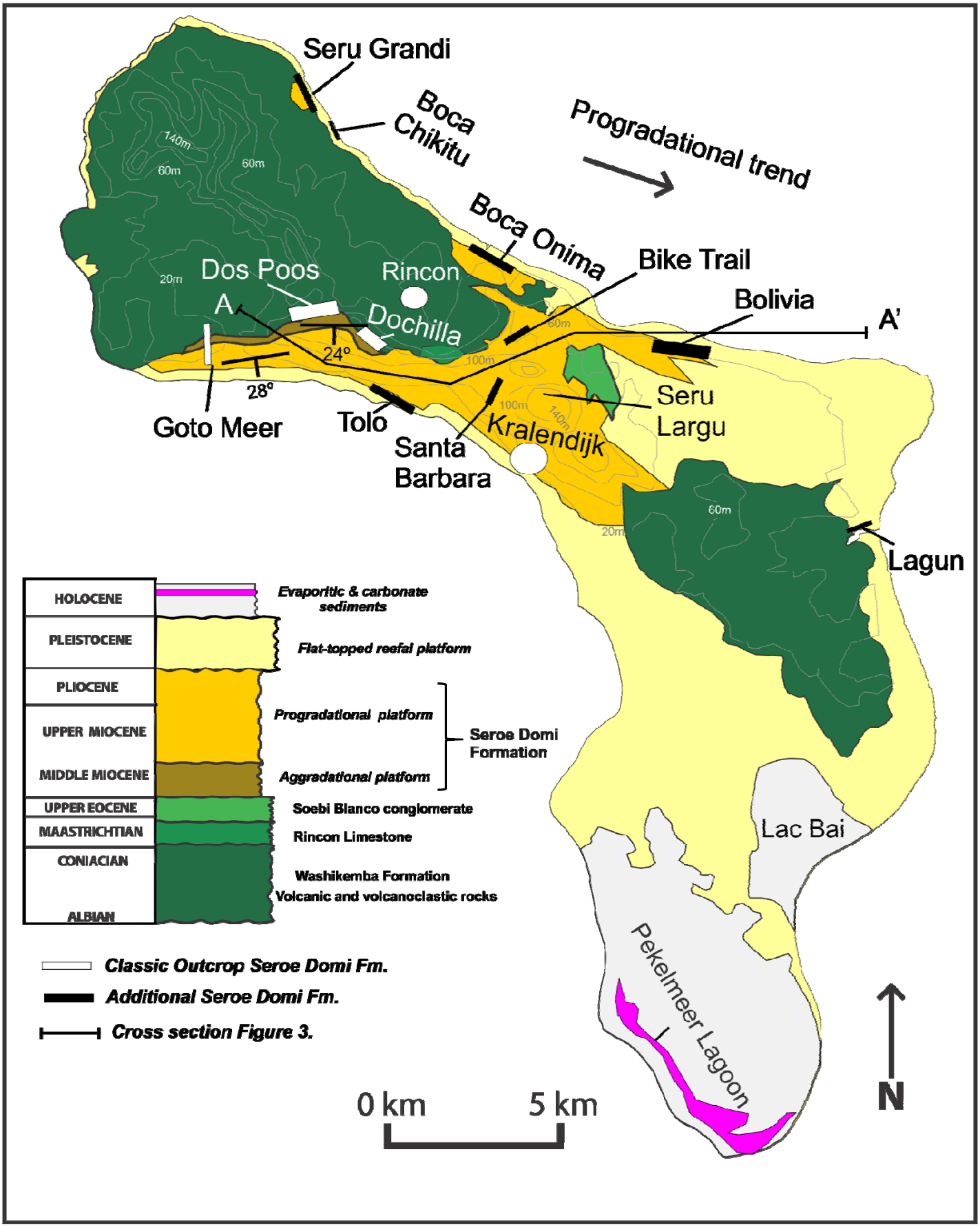

Figure 2: Geological map and stratigraphic column for Bonaire. Rectangles are study areas and ovals are major population centers. Modified from Hippolyte and Mann (2011).

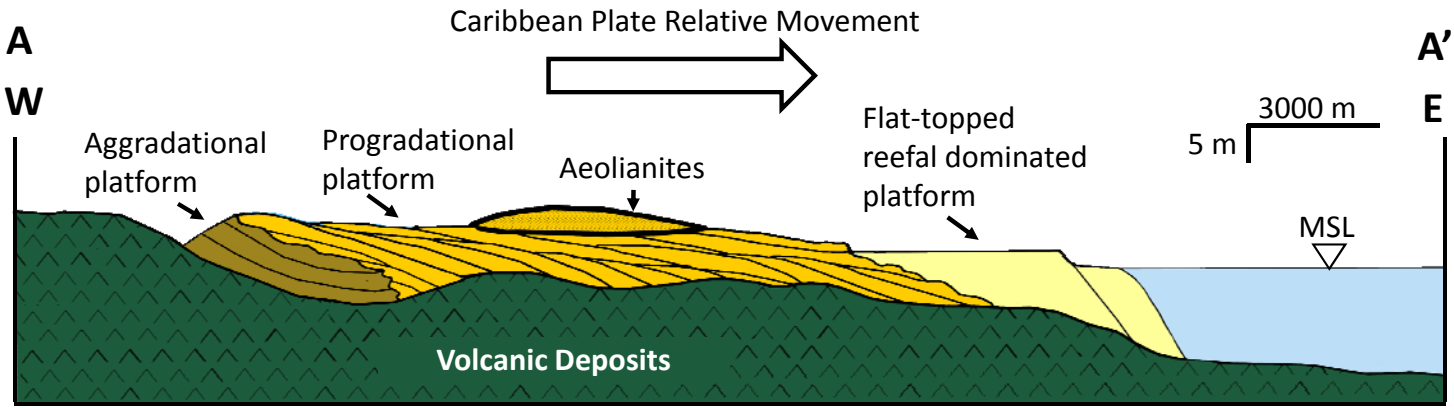

Figure 3: W-E schematic profile diagram showing the relationship of the three platforms episodes on Bonaire. Triangle indicates mean sea level (MSL).

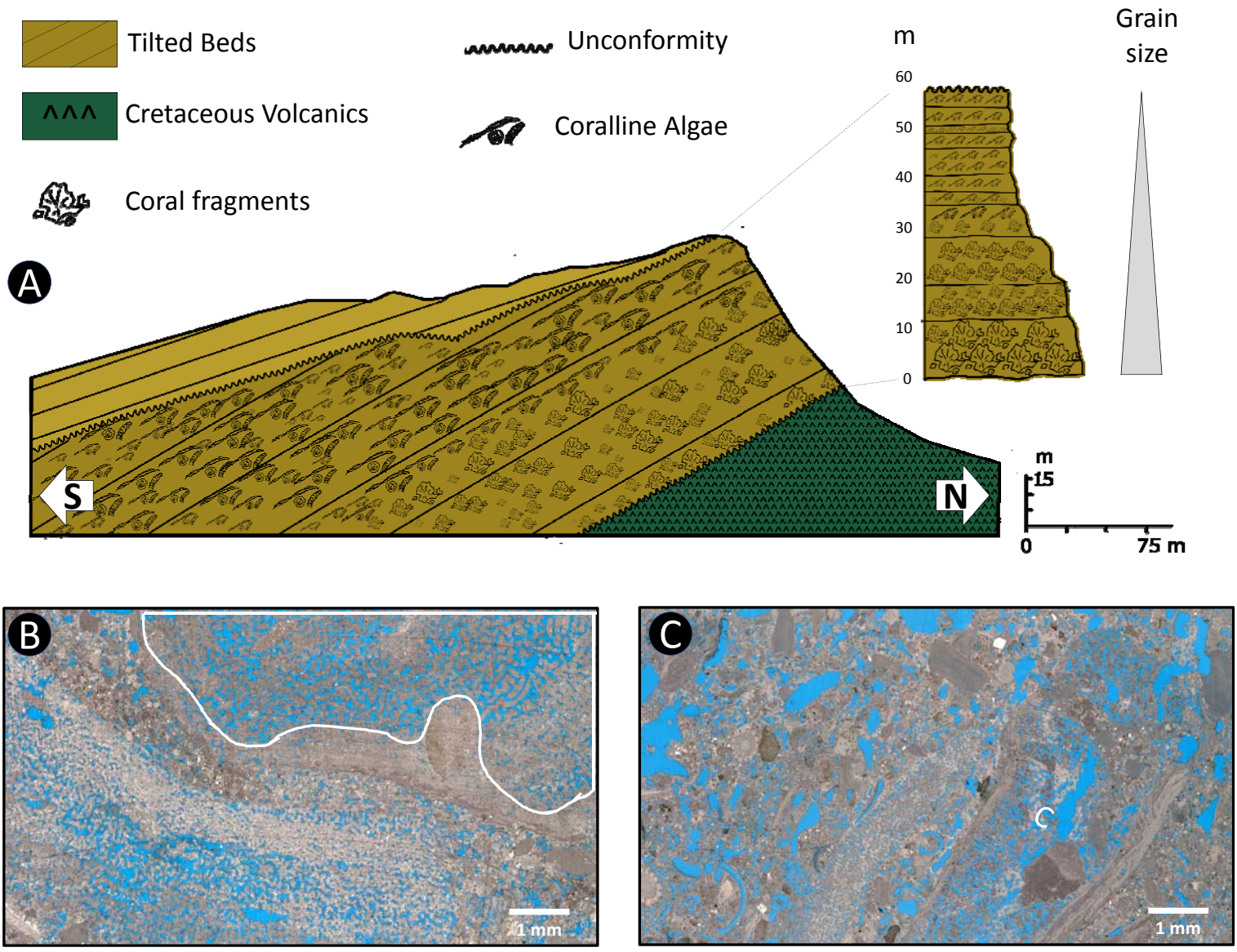

Figure 4: Stratal architecture and plane polarized light (PPL) thin-section photomicrographs of samples of the Mid-Miocene aggradational platform at Goto Meer, NW Bonaire. Blue is epoxy resin showing porosity. A) Interpreted Stratal architecture of the Mid-Miocene aggradational platform. B) Mixed coral rudstone grainstone facies (outlined) mixed with small fraction of foraminifera and shell fragments. C) Coralgal facies consisting of red algae, echinoderms, shell fragments and coral grains.

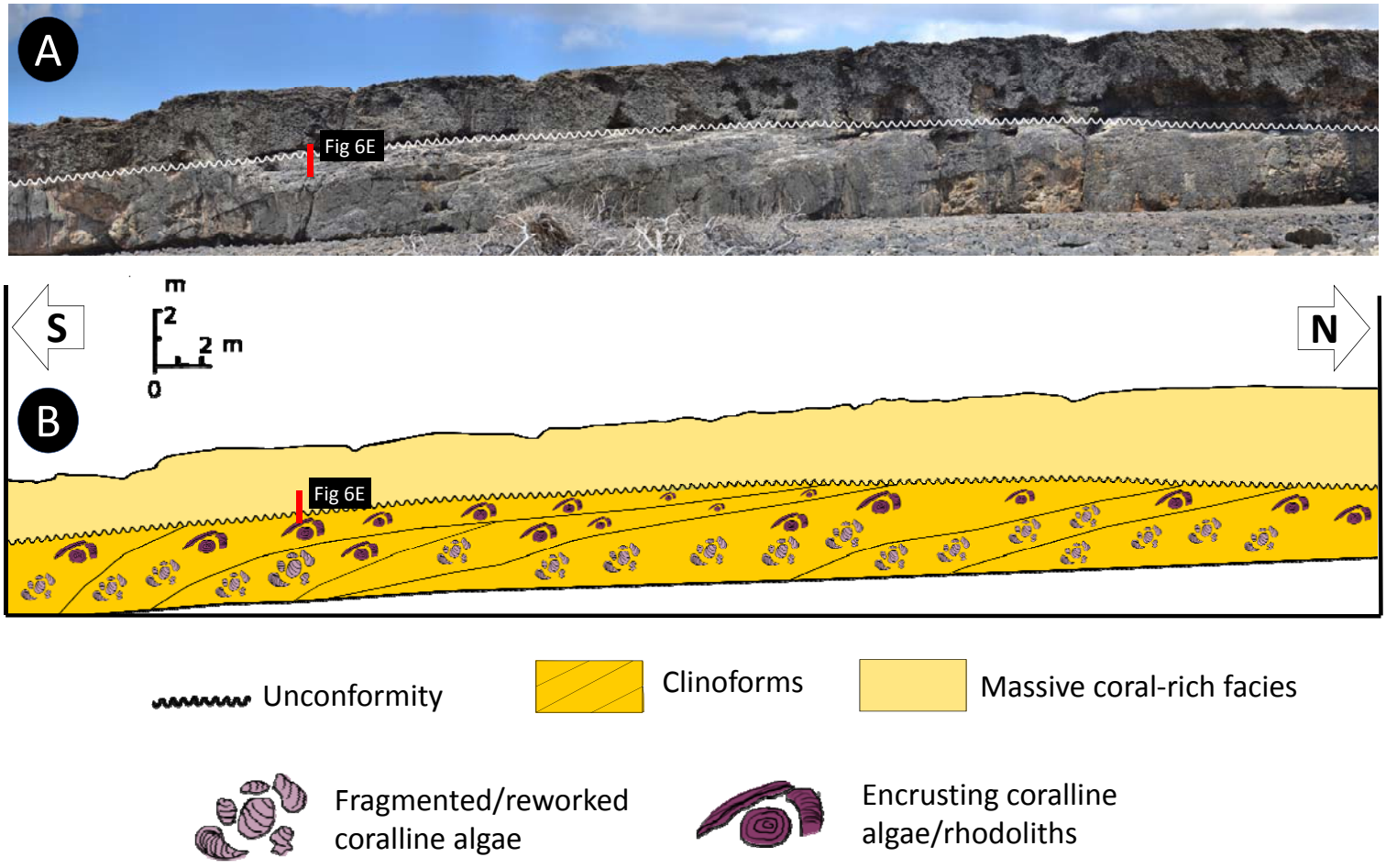

Figure 5: Seru Grandi outcrop showing the architecture of the prograding platform stage (Upper Miocene-Pliocene) and bioclast component distribution in the strata. Red bar represents the core sample location which shows the transition between underlying prograding platform stage and the overlying flat-topped platform stage (Figure 6).

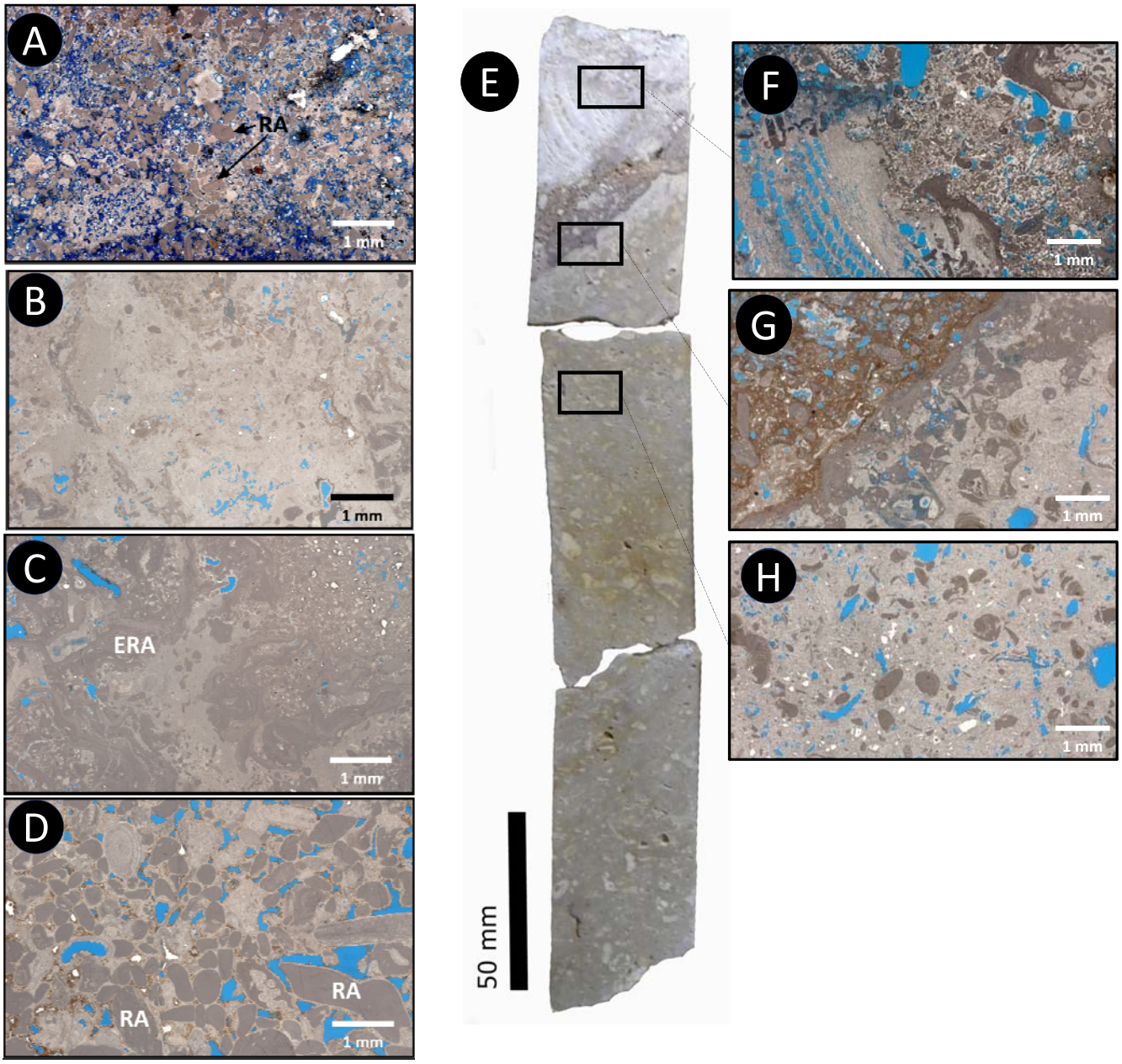

Figure 6: Plane polarized light images of thin sections and core sample of subfacies associated with prograding platform stage. Blue is epoxy resin showing porosity. A) Coralgal grainstone and packstone facies with abundant red algae (RA) fragments. B) Encrusting red algae (ERA) rich grainstone/packstone. C) Mimetic and partially fabric destructive dolomitized facies associated with red algae –rich packstone. D) Reworked red algal (RA) E) Core sample of the transition between underlying prograding platform stage and the overlying flat-topped platform stage. F) Coral fragments encrusted by red algae and reworked bioclastic material. grainstone/packestone. G) Unconformity/transition shown as darker material in upper left half of thin section, bordered by coralline red algae crust from the the underlying red algae rich prograding platform facies. H) Dolomitized red algal-rich facies characterized by mimetic structure and moldic porosity.

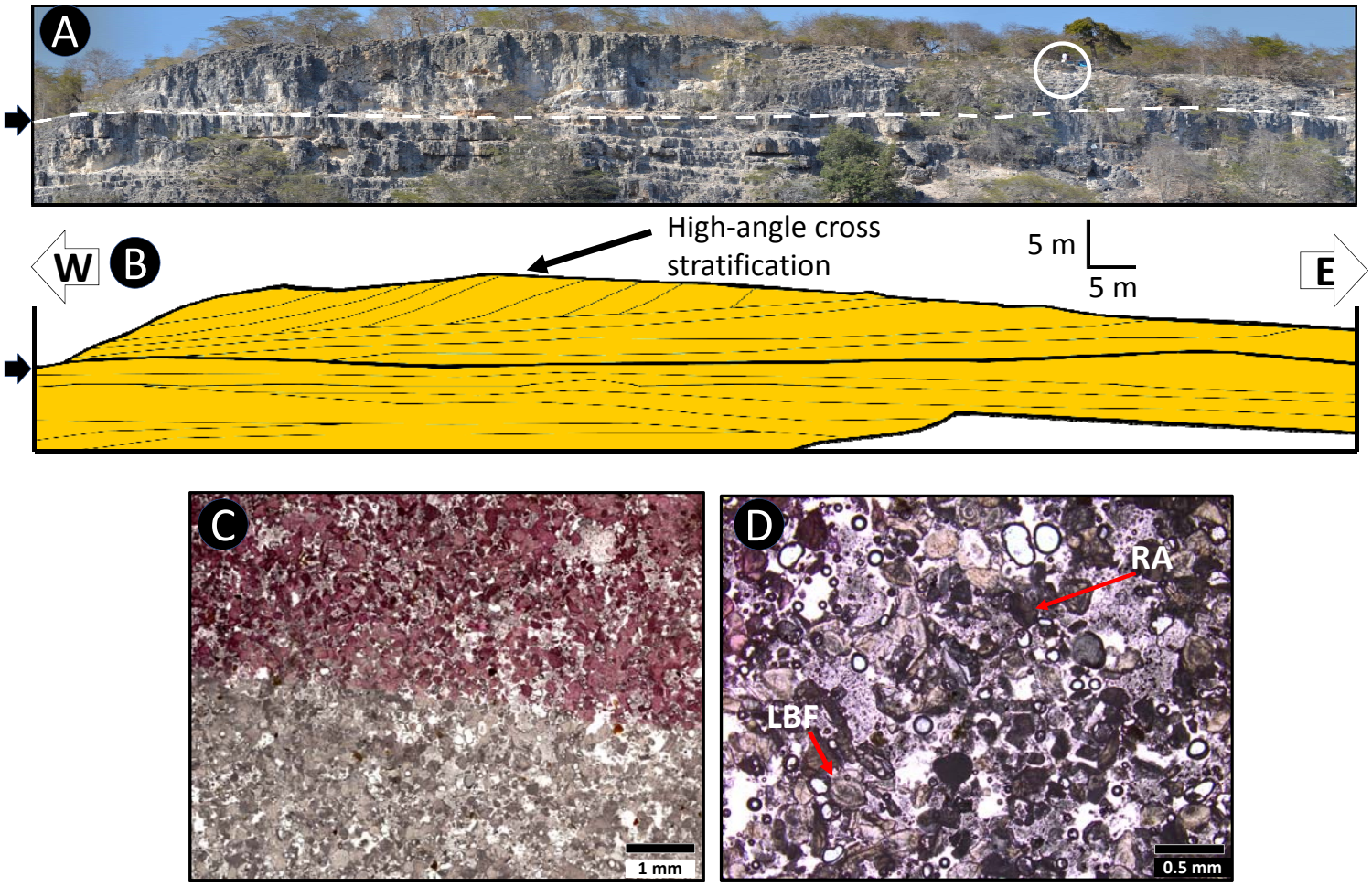

Figure 7: A) Aeolinite deposits with large scale cross stratification. Panoramic view of Seru Largu outcrop. White spots showing porosity. Note person for scale (circled). B) Schematic interpretation of the internal stratigraphic architecture. C) Thin section photomicrograph of dominant facies for this deposit comprisingLarge Benthic Foraminifera (LBF) and Red Algae (RA) grainstone main facies for this deposit. D) Zoomed-in view of C), highlighting skeletal composition of the aeolinite deposits.

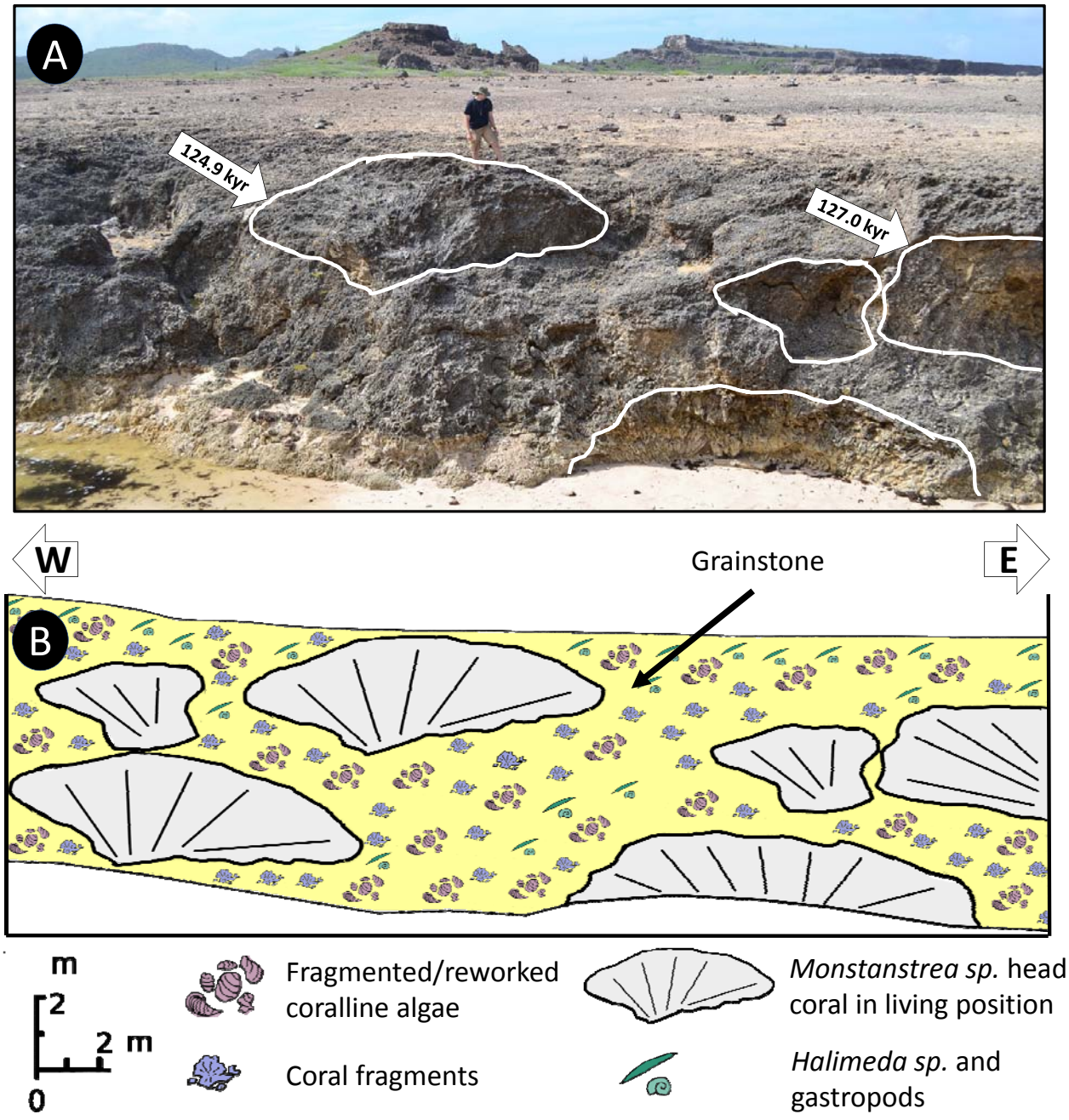

Figure 8: Field photo and schematic interpretation of Boka Chikitu outcrop. A) Reefal deposits showing flat-topped geometries, formed primarily of Monstastrea sp., of the Pleistocene flat-topped platform stage from Boca Chikitu. Arrow with ages of Monstastrea sp. heads acquired from U-Th dating. Seru Grandi (Figure 5) in background. B) Schematic interpretation of Monstastrea sp. amongst grainstones.

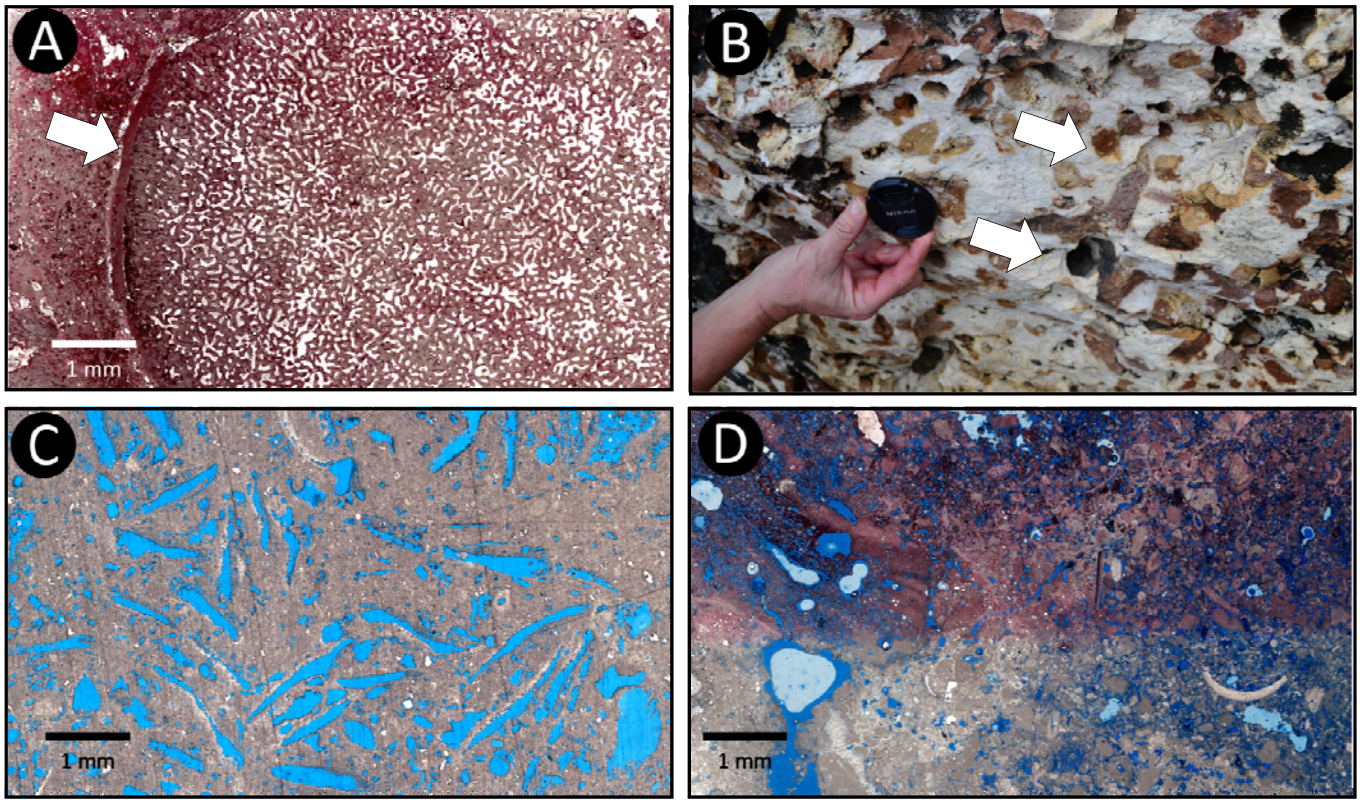

Figure 9: Plane polarized light images of thin sections (Blue is epoxy resin showing porosity) from Bolivia and an outcrop photo from Tolo. A) *Montastrea sp.* fragment showing well-defined internal structure. Note the contact between the coral fragment and bioclastic matrix (white arrow). B) *Acropora cervicornis* Floatstone. Note the reddish branching structures (arrows). C) Gastropod-green algae grainstone/packstone. D) Coralgal Grainstone/Packestone.

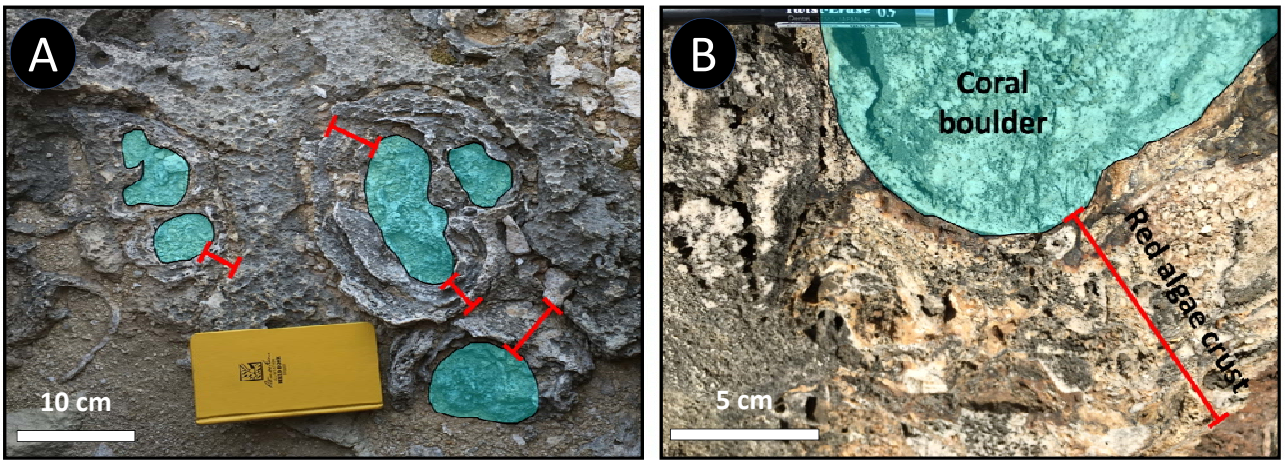

Figure 10: Coral-rich boulders mainly formed of *Montastrea sp.*, *Acropora palmata* and *Porites sp.* with red algal crust (A) encrustations can reach 10's of centimeter thick between boulders. (B) Close-up of coral boulder and red algae crust.

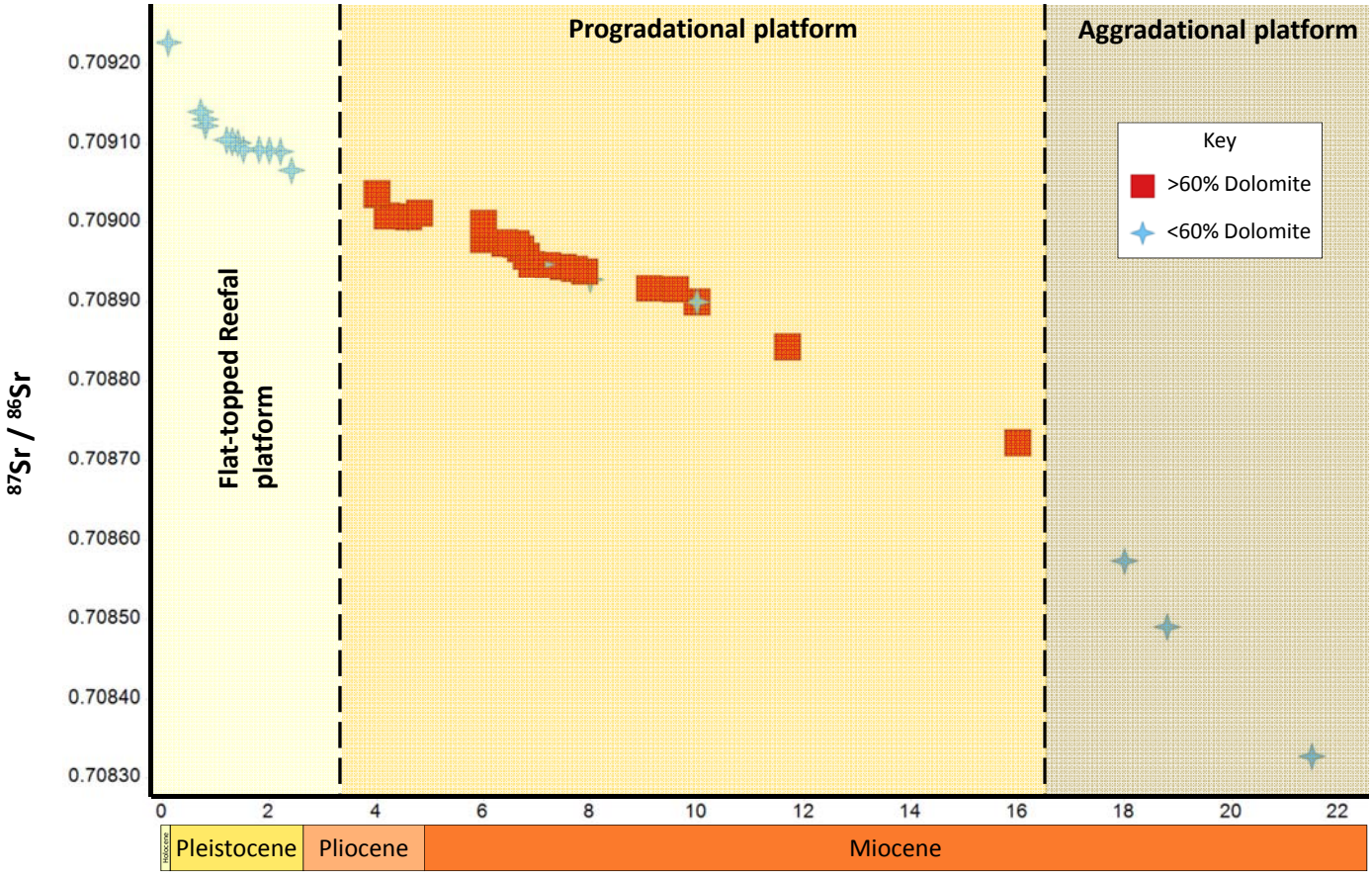

Figure 11: $^{87}Sr/^{86}Sr$ ratios curve of the three major facies. Age model for $^{87}Sr/^{86}Sr$ ratios based on McArthur et al. (2012). Red squares represent samples with more than 60% dolomite, blue stars represent samples with less than 60% dolomite.

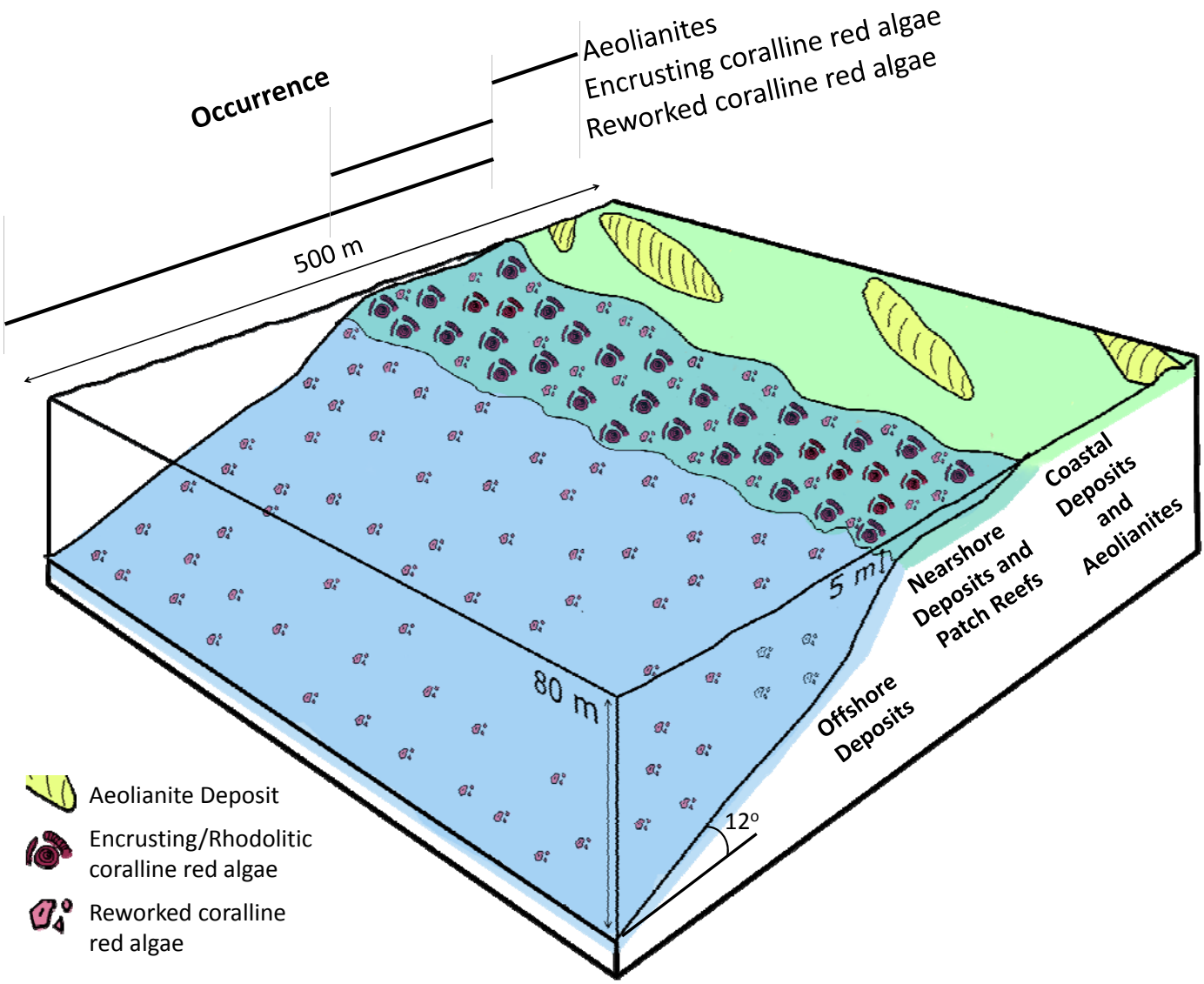

Figure 12: Schematic depositional environment diagram for the prograding (Upper Miocene-Pliocene) platforms.

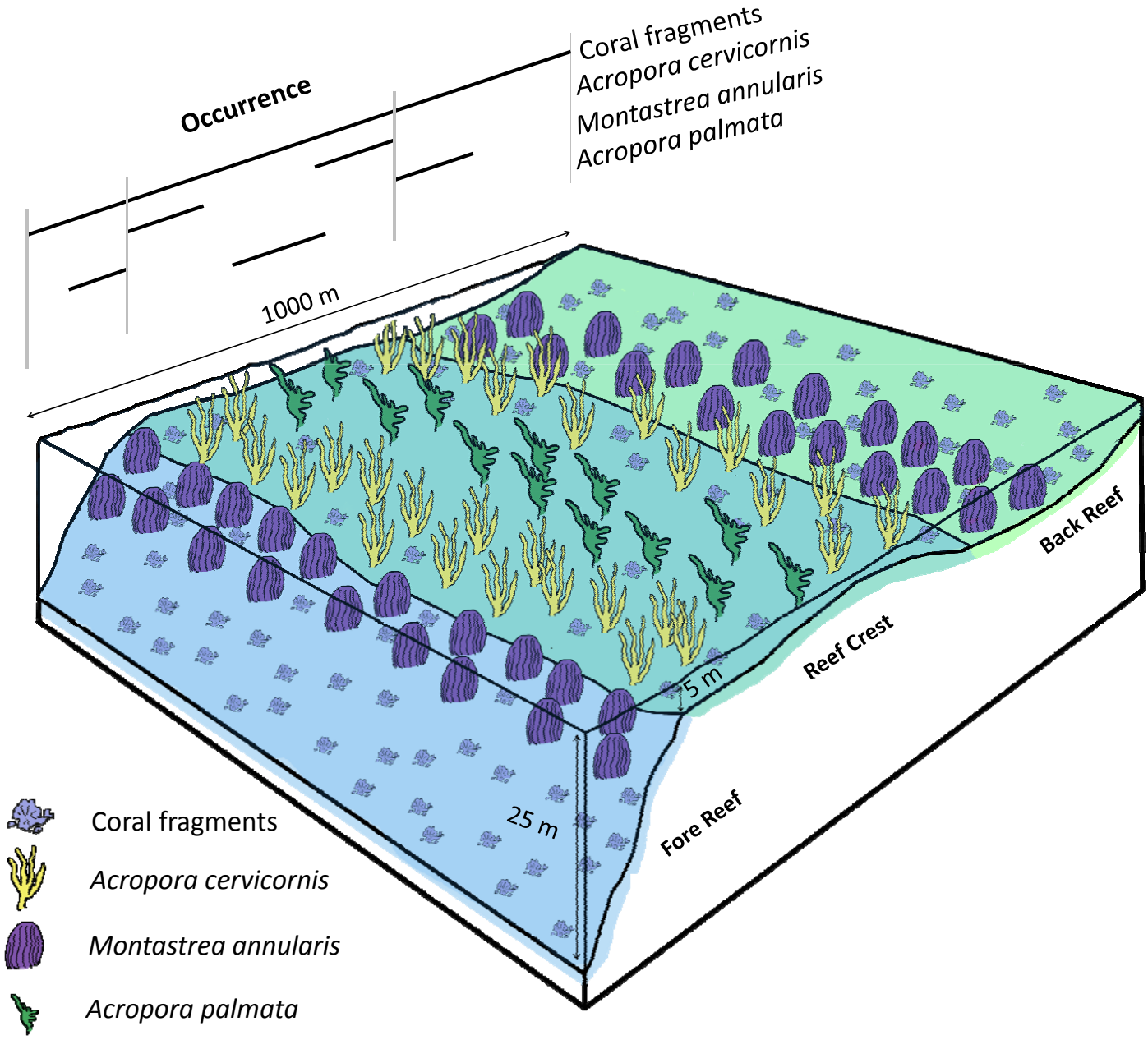

Figure 13: Schematic reefal facies distribution pattern for the flat-topped reefal (Pleistocene) platforms.

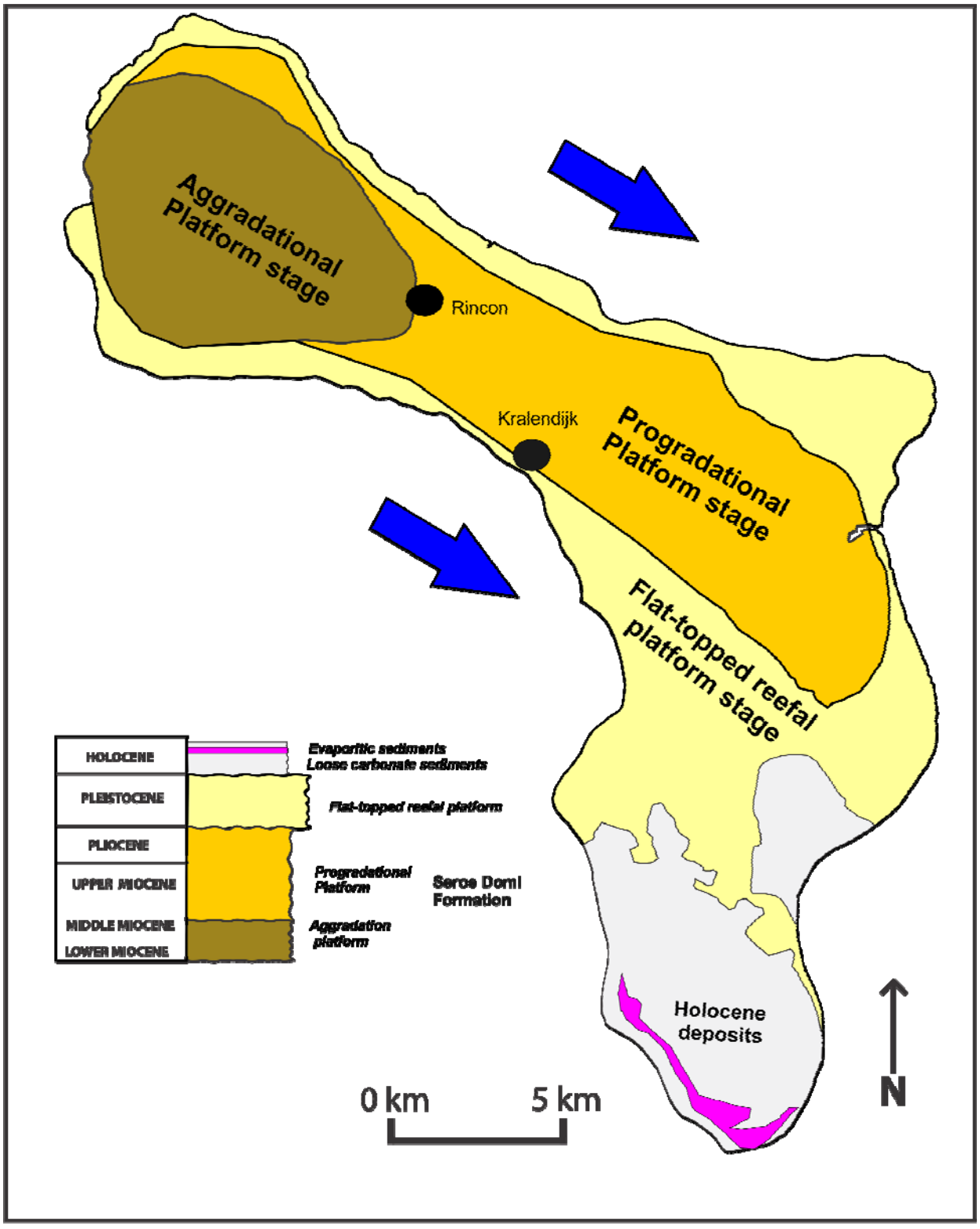

Figure 14: Map showing the distribution of platforms based on facies and Sr isotope dating ages, showing the broad-scale progradational pattern of Neogene carbonate deposition (blue arrows).

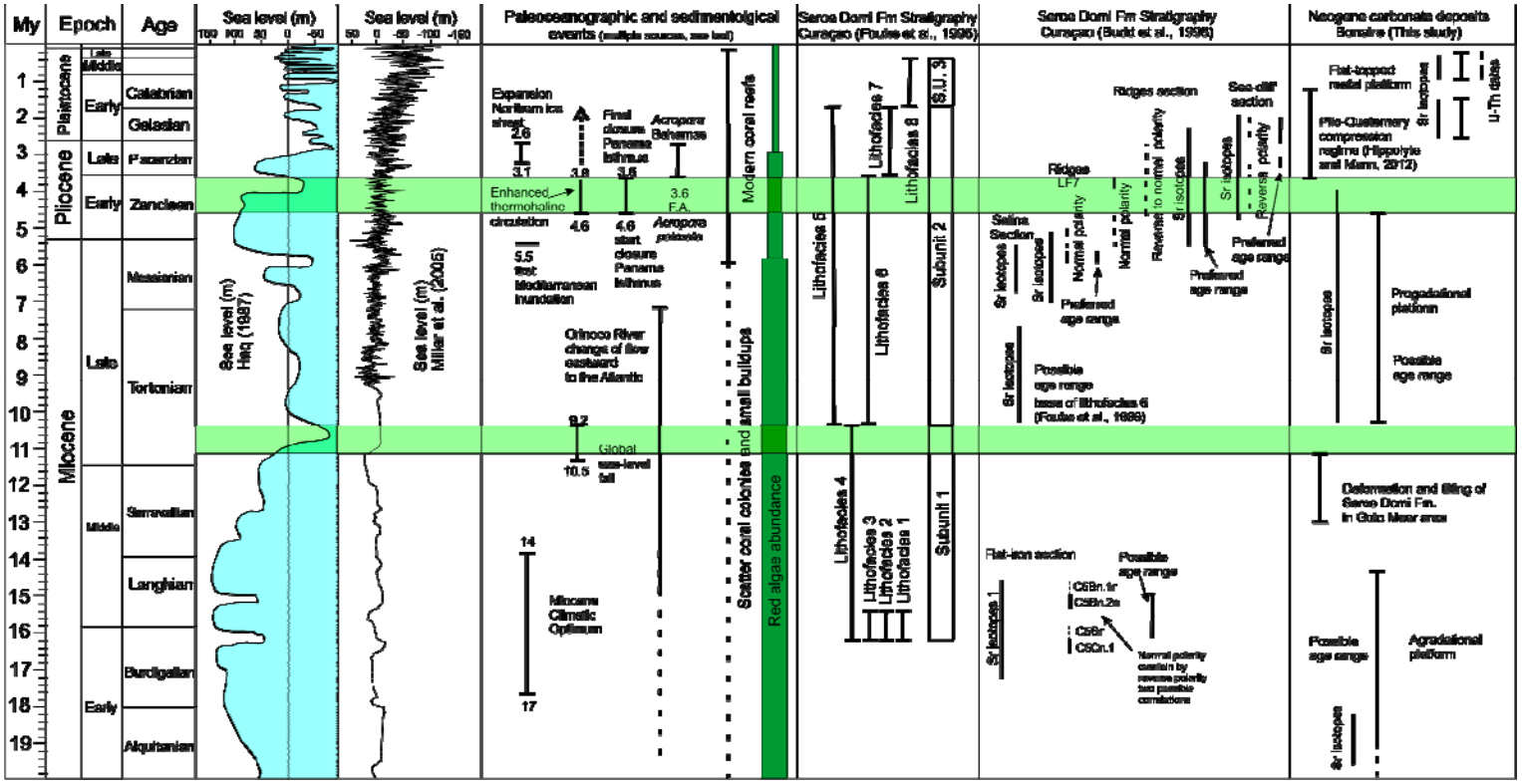

Figure 15: Chart of depositional, oceanographic and tectonic events that have contributed to the stratigraphic architecture of Bonaire. Green horizontal shades represent main environmental events which are concurrent with platform boundaries.